

**DEVELOPMENT OF ALUMINUM HONEYCOMB
CORED CARBON FIBER REINFORCED
POLYMER COMPOSITE BASED SANDWICH
STRUCTURES**

**A Thesis Submitted to
the Graduate School of Engineering and Sciences of
İzmir Institute of Technology
in Partial Fulfillment of the Requirements for the Degree of**

MASTER OF SCIENCE

in Mechanical Engineering

**by
Mehmet Ziya OKUR**

**December 2016
İZMİR**

We approve the thesis of **Mehmet Ziya OKUR**

Examining Committee Members:

Prof. Dr. Metin Tanođlu

Department of Mechanical Engineering, Izmir Institute of Technology

Doc. Dr. Engin Özçivici

Department of BioEngineering, Izmir Institute of Technology

Assist. Prof. Dr. Aylin Ziylan

Department of Metallurgical and Materials Engineering, Dokuz Eylül University

27 December 2016

Prof. Dr. Metin TANOĐLU

Supervisor, Department of Mechanical Engineering, İzmir Institute of Technology

Prof. Dr. Metin TANOĐLU

Head of the Department of Mechanical Engineering

Prof. Dr. Bilge KARAÇALI

Dean of the Graduate School of Engineering and Sciences

ACKNOWLEDGMENTS

I would like to thank and express my deepest gratitude to my advisor, Prof. Metin TANOĞLU for their invaluable advice, guidance, support and encouragement.

I am especially grateful to my laboratory colleagues and also, Research Assistants Bertan BEYLERGİL, Serkan KANGAL, Osman KARTAV, Mehmet Deniz GÜNEŞ and Zeynep AY for their encouragement, help and patience.

I would like express my appreciation to all my friends for their help, support and friendship.

Finally, I offer sincere thanks to my parents, Mustafa OKUR and Zeynep Nermin OKUR, and sisters for their endless patience and understanding during this thesis as in all stages of my life. I am also thankful to my fiancée Zeynep Şeyda AKYÜZ for their endless understanding, supports, motivation and love in all my life and believing in me. I am always sure that they are happy to be there for me. I cannot even imagine how much they contribute efforts for me.

ABSTRACT

DEVELOPMENT OF ALUMINUM HONEYCOMB CORED CARBON FIBER REINFORCED POLYMER COMPOSITE BASED SANDWICH STRUCTURES

Lightweight composite sandwich structures are composed of composite structures that are laminated between thin stiff facesheets bonded to a thicker lightweight core. These structures have high potential to be used in civil engineering applications, marine, aerospace industry etc. applications due to their high strength to weight ratios and energy absorption capacity. In these structures, the bending loads are generally carried by the force couple formed by the face sheets while the shear loads are carried by the lightweight core materials. Main purpose of the core material is to provide a high moment of inertia. Therefore, under flexural loading, sandwich panels have higher specific mechanical properties relative to the monocoque structures. Also, the core resists transverse forces and stabilizes the laminates against global buckling and local buckling. The resulting structure provides increased buckling resistance and its rigidity.

In this study, sandwich composite structures were developed with carbon fiber reinforced polymer composite facesheets and the cores made by Aluminum (Al) based honeycomb with various thicknesses. Carbon fiber/epoxy composite facesheets were fabricated with non-woven unidirectional (UD) fabrics (with $0^{\circ}/90^{\circ}$ orientation) and epoxy resin by vacuum infusion technique. Al honeycomb layers were sandwiched together with carbon/epoxy facesheets using a thermosetting adhesive. Mechanical tests were carried out to determine the mechanical behavior of face sheets, aluminum cores and the composite sandwich structures. Effect of core thickness on the mechanical properties of the sandwich structures was investigated.

Keywords: Sandwich structures, carbon fiber, epoxy, aluminium honeycomb, mechanical properties, vacuum infusion.

ÖZET

ALÜMİNYUM BAL PETEĞİ ARA TABAKA İÇEREN KARBON ELYAF TAKVİYELİ POLİMER KOMPOZİT ESASLI SANDVIÇ YAPILARIN GELİŞTİRİLMESİ

Hafif kompozit sandviç yapılar, ince rijit yüzey plakaları arasına yerleştirilen daha kalın hafif ara tabakanın lamine edilmesiyle oluşmaktadır. Bu yapılar, ağırlıklarına oranla yüksek mukavemet ve enerji sönümleme kabiliyetlerinden dolayı inşaat mühendisliği uygulamaları, denizcilik, havacılık ve uzay endüstrisi gibi uygulamalarda yüksek kullanım potansiyeline sahiptirler. Bu yapılarda, genellikle eğilme yükü yüzey plakaları tarafından oluşturulan kuvvet çifti tarafından taşınırken, kayma yüklerini hafif ara tabaka malzemeleri taşır. Ara tabaka malzemesinin asıl amacı, yüksek bir atalet momenti sağlamaktır. Bu yüzden, eğilme yükleri altında sandviç paneller, monokok (tek kabuklu) yapılara oranla daha yüksek özgül mekanik özelliklere sahiptir. Ayrıca, ara tabaka yanal kuvvetlere karşı direnç göstermekte ve lamineleri global ve lokal burkulmalara karşı dengelemektedir. Ortaya çıkan yapı, eğilme direncinin ve rijitliğinin artmasını sağlamaktadır.

Bu çalışmada, karbon fiber takviyeli polimer kompozit yüzey (kabuk) tabakaları ve Alüminyum (Al) esaslı bal peteği geometrisine sahip farklı kalınlıklardaki ara tabakadan oluşan kompozit sandviç yapılar geliştirilmiştir. Karbon fiber/epoksi kompozit yüzey tabakaları ($0^{\circ}/90^{\circ}$ yönelimiyle) örgüsüz tek yönlü karbon fiber ve epoksi reçine ile vakum infüzyon yöntemiyle üretilmiştir. Alüminyum bal peteği tabakaları, karbon/epoksi yüzey plakaları ile birlikte termoset bir yapıştırıcı kullanılarak sandviç haline getirilmiştir. Yüzey plakaları, alüminyum ara tabakalar ve kompozit sandviç yapıların mekanik davranışlarını belirlemek için mekanik testler gerçekleştirilmiştir. Ara tabaka kalınlığının sandviç yapıların mekanik özelliklerine etkisi incelenmiştir.

Anahtar Kelimeler: Sandviç yapılar, karbon elyaf, epoksi, alüminyum bal peteği, mekanik özellikler, vakum infüzyon.

TABLES OF CONTENTS

LIST OF FIGURES	ix
LIST OF TABLES	xiii
CHAPTER 1. INTRODUCTION	1
CHAPTER 2. BACKGROUND	3
2.1. Definition of Sandwich Structures	4
2.2. Application Areas of Sandwich Structures	7
2.3. Behavior of Sandwich Structures	8
2.3.1 Failure modes in sandwich structures	9
2.4. Constituents of Composite Sandwich Structures	16
2.4.1. Face sheet Materials	17
2.4.1.1. Composite Face sheets	17
2.4.1.1.1. Face sheet Matrix Materials.....	17
2.4.1.1.2. Face sheet Reinforcement Materials.....	19
2.4.1.1.3. Manufacturing Methods of Polymer Matrix Composite (PMC's)	21
2.4.2. Core Materials	23
2.4.2.1 Honeycomb Structures	25
2.4.2.1.1. Manufacturing of the Honeycomb Core Structures	26
CHAPTER 3. EXPERIMENTAL.....	28
3.1. Materials	28
3.2. Manufacturing of Composite Sandwich Panels	28

3.3. Characterization Techniques	30
3.3.1. Honeycomb Core Material	30
3.3.1.1. Optical Microscopy.....	30
3.3.1.2. Flatwise Compression Test of Al Honeycomb Materials	30
3.3.2. Composite Face Sheet Material	31
3.3.2.1. Determining Fiber Volume Fraction.....	31
3.3.2.2. Tensile Test.....	32
3.3.2.3. Compression Test.....	32
3.3.2.4. Flexural Test	33
3.3.2.5. Interlaminar Shear Test	34
3.3.3. Composite Sandwich Structure	35
3.3.3.1. Flatwise Compression Test	35
3.3.3.2. Flatwise Tensile Test	35
3.3.3.3. Edgewise Compression Test	36
3.3.3.4. Flexural Test	37
3.3.3.5. Mode I Interfacial Peel Strength Test	39
 CHAPTER 4. RESULTS AND DISCUSSIONS.....	 40
4.1. Properties of Al Honeycomb Core Materials	40
4.1.1. Cell Wall Thickness.....	40
4.1.2. Flatwise Compression Properties	41
4.2. Properties of Face Sheet Material	44
4.2.1. Fiber Volume Fraction.....	44
4.2.2. Tensile Test Results	44
4.2.3. Compression Test Results.....	46
4.2.4. Flexural Test Results	47

4.2.5. Interlaminar Shear Strength (ILSS) of the composite	48
4.3. Mechanical Behavior of Composite Sandwich Structures	49
4.3.1. Flatwise Compressive Behavior of Sandwich Structures	49
4.3.2. Flatwise Tensile Behavior of Sandwich Structure	53
4.3.3. Edgewise Compression Test of the Sandwich Structures	56
4.3.4. Flexural Test Result of the Sandwich Structure	61
4.3.5. Mode-I Interfacial Peel Strength Values	65
CHAPTER 5. CONCLUSION.....	69
REFERANCES	71

LIST OF FIGURES

<u>Figure</u>	<u>Page</u>
Figure 2.1. Schematic diagram showing the construction of a sandwich panel	4
Figure 2.2. Efficiency of the sandwich structure	5
Figure 2.3. The construction of a sandwich panel compared to an I beam.....	6
Figure 2.4. Typical failure modes of sandwich panels	9
Figure 2.5. Examples of the three forms of honeycomb shown as core structures in sandwich panels: (a) hexagonal honeycomb, (b) square honeycomb and (c) triangular honeycomb	26
Figure 2.6. Honeycomb manufacture by the expansion process	27
Figure 2.7. Honeycomb manufacture by the corrugation process	27
Figure 3.1. Nomenclature of the hexagonal honeycomb core material	28
Figure 3.2. Flow chart of composite sandwich structure manufacturing	29
Figure 3.3. Flatwise compression test specimen (Al honeycomb core) under loading ..	30
Figure 3.4. Tensile test specimen (composite face sheet) during the test	32
Figure 3.5. Flexural test specimen (composite face sheet) under loading.	33
Figure 3.6. SBS test specimen and test configuration	34
Figure 3.7. Flatwise tensile test specimen (Carbon fiber/epoxy composite/Al honeycomb sandwich) and test configuration.....	35
Figure 3.8. Edgewise compression specimen (Carbon fiber/epoxy composite/ Al honeycomb sandwich) under loading	36
Figure 3.9. Three point bending test specimen (Carbon fiber/epoxy composite/Al honeycomb sandwich) under loading	37
Figure 3.10. Sandwich structure dimensions	38
Figure 3.11. Peel test specimen under loading to determine interfacial properties	39
Figure 4.1. Optical microscope images of Al core material cross-sections for (a) 6 mm, (b) 21 mm and (c) 46 mm thick cores (magnification: 20X).....	40
Figure 4.2. Force-displacement curves of Al based honeycomb core materials under flatwise compression (core thickness is 6 mm)	41
Figure 4.3. Force-displacement curves of Al based honeycomb core materials under flatwise compression (core thickness is 21 mm)	41

Figure 4.4. Force-displacement curves of Al based honeycomb core materials under flatwise compression (core thickness is 46 mm)	42
Figure 4.5. Comparison of typical flatwise compressive behavior of Al based honeycomb core materials for various core thicknesses	42
Figure 4.6. Images of flatwise compression test specimens; before (a-c-e) and after	43
Figure 4.7. Stress-strain curves of carbon/epoxy composite face sheets under tensile loading.....	45
Figure 4.8. Tensile test specimen and set-up (left) and the failed test specimen (right)	45
Figure 4.9. Stress-strain curves of composite face sheets under compression	46
Figure 4.10. The images of the compression test set-up (left) and the test specimen after compressive loading (middle, right)	46
Figure 4.11. Flexural stress-strain curves of composite face sheet under three-point bending.....	47
Figure 4.12. The images of flexural test specimen (a) before and (b) after bending test	48
Figure 4.13. Force-displacement curves of composite sandwich structure under flatwise compression (Al honeycomb core thickness is 6 mm)	50
Figure 4.14. Force-displacement curves of composite sandwich structure under flatwise compression (Al honeycomb core thickness is 21 mm)	50
Figure 4.15. Force-displacement curves of composite sandwich structure under flatwise compression (Al honeycomb core thickness is 46 mm)	51
Figure 4.16. Typical force-displacement curves of composite sandwich structures for various core thicknesses obtained from the flatwise compression tests	51
Figure 4.17. The images of flatwise compression test samples of the composite sandwich structures; before (a-c-e) and (b-d-f) after the tests (C: crushing, CB: core buckling) (t is core thickness in mm)	52
Figure 4.18. (a) Collapse sequence images and (b) representative force-displacement curve and the specific absorbed energy ($E_{s,a}$), graph of the composite sandwich structures under flatwise compression (core thickness is 46 mm)	53
Figure 4.19. Force-displacement curves of the composite sandwich structures under flatwise tension (core thickness is 6 mm)	54
Figure 4.20. Force-displacement curves of the composite sandwich structures under flatwise tension (core thickness is 21 mm)	54

Figure 4.21. Force-displacement curves of the composite sandwich structures under flatwise tension (core thickness is 46 mm)	55
Figure 4.22. Images of flatwise tensile test specimen of the composite sandwich structures; before (a-c-e) and (b-d-f) after the tests (Interfacial failure region within the specimens are visible) (t: core thickness in mm)	55
Figure 4.23. Force-displacement curves of the composite sandwich structures under edgewise compression (core thickness is 6 mm)	56
Figure 4.24. Force-displacement curves of the composite sandwich structures under edgewise compression (core thickness is 21 mm)	57
Figure 4.25. Force-displacement curves of the composite sandwich structures under edgewise compression (core thickness is 46 mm)	57
Figure 4.26. Comparison of typical edgewise compressive behavior of the composite sandwich structures for various core thicknesses	58
Figure 4.27. Images of edgewise compression test specimens; before (a-c-e) and after (b-d-f) the tests (CC: core crushing, GB: global buckling, DB: debonding) (t is the thickness of the core in mm)	60
Figure 4.28. Force-displacement curves of composite sandwich structures under flexural loading (core thickness is 6 mm)	62
Figure 4.29. Force-displacement curves of composite sandwich structures under flexural loading (core thickness is 21 mm)	62
Figure 4.30. Force-displacement curves of composite sandwich structures under flexural loading (core thickness is 46 mm)	63
Figure 4.31. Comparison of typical flexural behavior of composite sandwich structures for various core thicknesses	63
Figure 4.32. Images of flexural test specimens; before (a-c-e) and after (b-d-f) the tests (DB: debonding, CC: core crushing and D: delamination) (t is the core thickness in mm)	64
Figure 4.33. Force-displacement curves of composite sandwich structures under peel loading (core thickness is 6 mm)	65
Figure 4.34. Force-displacement curves of composite sandwich structures under peel loading (core thickness is 21 mm)	65
Figure 4.35. Force-displacement curves of composite sandwich structures under peel loading (core thickness is 46 mm)	66

Figure 4.36. Mode-I peel test specimens; at the beginning (a-c-e) and during (b-d-f) the tests (t is the core thickness in mm) 67

Figure 4.37. SEM fracture surfaces images of Mode-I test specimens; (a) the face sheet side, and (b) the core side of the specimen. 68

LIST OF TABLES

<u>Table</u>	<u>Page</u>
Table 3.1. Specimen dimensions for edgewise compression test	37
Table 4.1. Summary of flatwise compression test results	43
Table 4.2. Fiber volume fraction of face sheets manufactured	44
Table 4.3. Summary of tensile properties of carbon/epoxy composite face sheets	45
Table 4.4. Summary of compression test results of carbon/epoxy composite	47
Table 4.5. Summary of flexural test results for carbon/epoxy composite	48
Table 4.6. Summary of ILSS test results of carbon/epoxy composite	48
Table 4.7. Summary of flatwise compression test results for carbon-epoxy/Al honeycomb composite sandwich structures with various core thicknesses ...	52
Table 4.8. Summary of flatwise tensile test results for composite sandwich structures with various core thicknesses	56
Table 4.9. The ultimate edgewise compressive strength and specific absorbed energy, $E_{s,a}$ of the composite sandwich structures with different core thickness	59
Table 4.10. Summary of the flexural test results of the composite sandwich structures	64
Table 4.11. Summary of Mode-I fracture toughness tests	66

CHAPTER 1

INTRODUCTION

Composite sandwich structures have been used in many applications ranging from satellites, aircraft, ships, automobiles, rail cars, wind energy systems to bridge construction due to their light weight, high flexural and transverse shear stiffness, and corrosion resistance (Vinson 2005 and Hasseldine, et al. 2015). Moreover, these structures are capable of absorbing large amounts of crash energy in the event of a sudden collision (Mamalis, et al. 2005).

A composite sandwich structure is composed of a thick, lightweight and compliant core material sandwiched between two stiff and high strength face sheets. The performance of the whole sandwich structures is related to the properties of the constituents and they can be effectively manufactured by lamination, offering unique and valuable structure-property options to designers (Shi, et al. 2014). There are mainly two different classes of cores such as; foams and honeycombs, with a wide range of materials and properties within each type. Face sheets are commonly made of laminated fiber reinforced plastics or can be metallic or fully plastic (Aktay, et al. 2008).

In a sandwich structure, the bending loads are generally carried by the force couple formed by the face sheets while the shear loads are withstood by the lightweight core materials. The face sheets are strong in tension and compression, as compared to the low-density core material whose primary reason is to provide a high moment of inertia. The low-density of the core material results in low panel density, under flexural loading subsequently. Sandwich panels have higher specific mechanical properties relative to the monocoque structures. Hence, sandwich panels are exceptionally adequate in carrying bending loads. Under flexural loading, face sheets form a force couple so that one laminate is under compression and the other is under tension. Thus, the core resists transverse forces and stabilizes the laminates against global buckling and local buckling. The resulting structure provides increased buckling and crippling resistance to shear panels (Donga 2011, Adams 2006). In addition, the composite action is defined as the ratio between the bending moment of the couple and the overall bending moment. In general, the bending resistance of the panel is totally resisted by the

couple when no localized loads are involved. In case of localized effects, additional local bending moments in the face sheets and high interfacial stresses between the face and core may occur which reduces the contribution of the couple to the over bending moment resistance or the composite action (Frostig 2005).

The dominant properties of sandwich structures change subjected to the application area of the structure. For instance, in automotive industry, the out-of-plane compressive properties are more critical, whereas in wind turbines, the in-plane compressive properties are more pronounced. Therefore, depending on the application area, different properties or characteristics of sandwich panels need to be evaluated (Donga 2011).

The aim of this study is to develop manufacturing routes of carbon fiber reinforced polymer (CFRP) face sheet/aluminum (Al) core based sandwich structures and investigate the mechanical behavior of those structures with various core thicknesses. For this purpose, CFRP composite face layers were fabricated by vacuum infusion technique. Composite face and Al core materials were laminated together by an adhesive joining technique. Flatwise compression (FC), Flatwise Tensile (FT), Edgewise compression (EC), Mode I peel strength and flexural bending (3PB) tests were applied on composite sandwich specimens. Constituents of the sandwich structures were also tested mechanically and a conclusion is drawn for an optimized sandwich structures.

CHAPTER 2

BACKGROUND

Composite material can be defined as a combination of two or more materials that results in preferable properties over those of the individual components used alone. In contrast to metallic alloys, each material retains its separate chemical, physical, and mechanical properties. Generally, the two constituents are reinforcement and matrix. The main advantages of composite materials are their high strength and stiffness, combined with low density, when compared with monolithic materials, allowing for a weight reduction in the finished part (Campbell 2010). Composites have unique advantages such as high strength and stiffness, low density, long fatigue life and adaptability to the intended function of the structure. They offer further improvements in corrosion resistance, wear resistance, appearance, temperature-dependent behavior, thermal stability, thermal insulation, thermal conductivity and acoustic insulation. The reasons are their high specific strength and stiffness due to the low density and the anisotropic and heterogeneous character of the material. The anisotropic and heterogeneous characteristics also provide freedom to design a structure with optimum configuration for serving a specific function (Daniel and Ishai 1994).

Composite materials can be classified into three main categories; (i) particle-reinforced, (ii) fiber-reinforced, and (iii) structural composites. In particle-reinforced composites, which are composed of macro size particles of one material in a matrix of another and this particulate phase is harder and stiffer than the matrix. Fiber-reinforced composites consist of fibers of one material in a matrix material of another (Reddy 2004). Also the dispersed phase has the geometry of a fiber, the mechanical properties mostly depend on the properties of the fibers and applied load is transmitted to the fibers by the matrix phase through the fiber/matrix interface. Structural composites are the combinations of composites and homogeneous materials and the geometrical design of the structural elements affect the mechanical properties of the structure. The most common structural composites are laminated composites and sandwich panels (Callister 2006).

2.1. Definition of Sandwich Structures

Sandwich panels, a class of structural composites, are designed to be lightweight beams or relatively stiff and strength panels. A sandwich panel is composed of two outer sheets, or faces which adhesively bonded to a thicker core (Figure 2.1). The outer sheets are made of a relatively stiff and strong material, typically fiber-reinforced plastics, aluminum alloys, steel, titanium or plywood; they impart high stiffness and strength to the structure, and must be sufficiently thick to resist tensile and compressive stresses that result from loading. The core material is lightweight and normally has a low modulus of elasticity. Core materials typically fall within three categories: rigid polymeric foams such as; phenolic, epoxy, polyurethanes, wood and honeycombs (Callister 2006). The construction of honeycomb structure is shown in Figure 2.1.

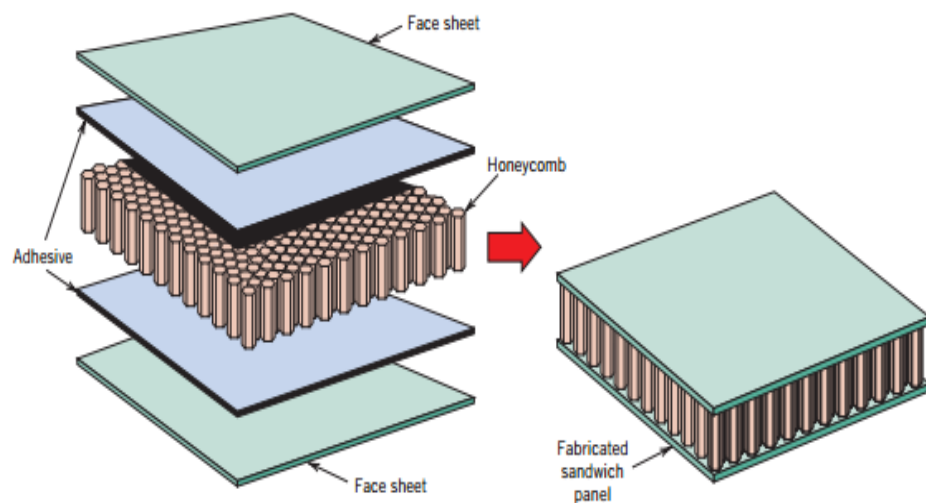


Figure 2.1. Schematic diagram showing the construction of a sandwich panel
(Source: Callister 2006)

Face sheets in structural sandwiches possess usually same material and thickness and they primarily resist in-plane and bending loads. These structures are called symmetric sandwich structures while asymmetric sandwich structures have the face sheets vary in thickness or material depending on certain special cases such as different loading conditions or working environment. Sandwich structures generally are symmetric and the diversity of sandwich structures are particularly linked with the core configuration. Any material or architecture can be used in the sandwich structures as a

core material, but they are generally classified in four categories, honeycomb core, foam or solid core, corrugated or truss core and web core. Another important criterion is the adhesion of face sheets and core. Because the functioning of the sandwich structure as a whole and also the load transfer depend on the adhesion quality of face sheets and core (Rao and Rao 2014).

Each component in sandwich structures is subjected to different loading conditions so that face sheets carry the in-plane and bending loads while the core resists the shear loads. The face sheet material usually has a high stiffness as well as strong and thin, whereas, soft but thick core typically has low density, high compressive and shear strength. When these are bonded together, this combination provides the sandwich structure a high flexural modulus (Vinson 1999, Vrabie and Chiriac 2014). In addition, these structures offer higher capacity of stiffness with a few weight increments. Figure 2.2 shows the difference between a monolithic or laminated plate and a sandwich one concerns the presence of a low density cellular solid (Catapano and Montemurro 2014).


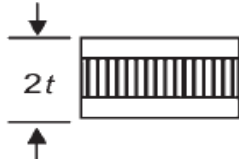
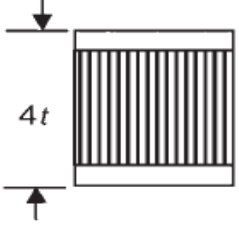
	Solid Material	Sandwich Construction	Thicker Sandwich
			
Stiffness	1.0	7.0	37.0
Flexural Strength	1.0	3.5	9.2
Weight	1.0	1.03	1.06

Figure 2.2. Efficiency of the sandwich structure.
(Source: Campbell 2010)

Sandwich construction is extremely efficient structural rigidity, especially in critical applications. As shown in Figure 2.2, doubling the thickness of the core increases the stiffness over seven times with only a three percent weight gain, while quadrupling the core thickness increases stiffness over 37 times with only a six percent

weight gain. Structural designers are intended to use sandwich construction whenever possible. Sandwich panels are typically used for their structural, electrical, insulation, and/or energy absorption characteristics (Campbell 2010).

Face sheets support almost all of the tension, compression, or bending loads. On the contrary, the core material with low density provides most of the through-the-thickness shear resistance and stabilizes the face sheets usually through adhesive bonding and this core material dramatically increases the moment of inertia keeping at a certain distance from the neutral axis of the sandwich panel. Moreover, they lead to higher buckling and crippling resistance to shear planes. These structures are more desirable than other constructions due to their lightweight, high specific bending stiffness and strength under distributed loads as well as their good energy absorbing capacity (Zhou et al. 2006 and Adams 2006).

The face skins of a sandwich panel can be considered as the flanges of an I-beam (Figure 2.3), because they carry the bending stresses in which the panel is subjected with one facing skin in compression, and the other in tension. Similarly, the core corresponds to the web of the I-beam (Paik et al. 1999). The core cannot withstand high tensile or compressive loads. However, it has several functions; first of all, it provides continuous support for the faces. Secondly, the core allows the whole structure to behave as one unit with high torsional and bending rigidity. In addition, it must have sufficient shear strength to resist transverse shear stresses, and also be thick enough to provide high shear stiffness in order to withstand buckling of the panel. It should be noted that tensile and compressive stresses on the core are much lower than on the faces (Callister 2006)

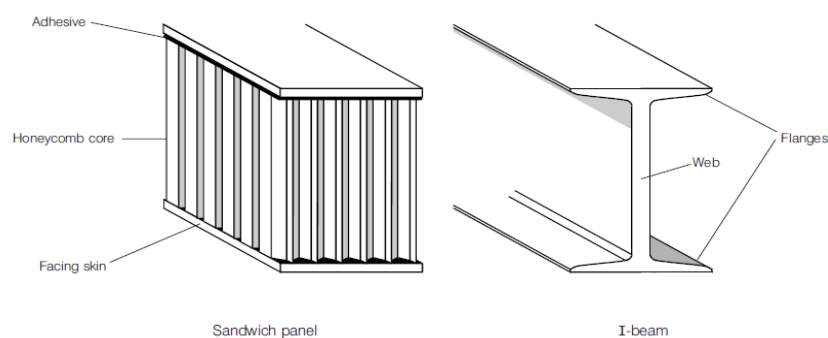


Figure 2.3. The construction of a sandwich panel compared to an I beam
(Source: HexWebTM, 2000)

Some of the basic structural requirements should be satisfied, if a sandwich panel is desired to have better performance. The skins must be thick enough to withstand tensile and compressive stresses induced by the design load and the core must have sufficient shear strength to withstand shear stresses design load. Also, the core must have enough thickness and sufficiently high shear modulus to prevent overall buckling of the sandwich. Also, the core material must have high modulus as well as high compressive strength to prevent wrinkling of the skins under the design load. In addition, cells in the core must be small enough to prevent dimpling of the skins under the design load (Mallick 1997). The resulting sandwich panel is strong enough to bear these stresses. Thus, the behavior of the sandwich panel in bending is considered to be critical for intended applications of thin polymer composite (Bari and Bajaj 2014).

2.2. Application Areas of Sandwich Structures

Recently, the use of structural sandwich composites have been increased in many applications such as aircraft structures, ship hulls, wind turbine blades, bridge decks due to their superior bending stiffness, low weight, and excellent thermal insulation and acoustic damping (Atas and Potoglu 2016). These structures are popular in high performance applications where weight reduction is important i.e. aeronautical structures, high speed marine craft and racing cars. Generally, the skins are made of composite materials. Cheaper alternatives such as aluminum alloy steel or plywood are also commonly used. Materials used for cores include polymers aluminum wood and composites. The cores are used in the form of foams, honeycombs or with a corrugated construction to minimize weight of the structure (Petras 1998). Decreasing weight of the vehicles provides fuel economy. The usage of the composite sandwich structures in aerospace and automotive industries becomes more popular because of their extremely low weight, high flexural and transverse shear stiffness and corrosion resistance. Moreover, sandwich structures are suitable in crashworthiness applications exhibit high energy absorption capacity when it suddenly subjected to impact loads (Donga 2011). Sandwich panels are also promising materials for using in several structural engineering applications such as flooring, decking, roofing and cladding panels. The main function of the exterior cladding is to provide shelter from weather conditions (rain, snow and

wind etc.) as well as providing the necessary thermal insulation. The most important design criterion in this case is to resist and transfer wind loads on the internal skeleton of the building. The conventional exterior cladding is usually made of different types of sandwich panels. These are reinforced concrete sandwich panels and the corrosion of steel reinforcement in these panels is the main issue (Sharaf 2010).

2.3. Behavior of Sandwich Structures

Critical characteristics of a sandwich structure depend on the loading conditions in real-case applications. For instance, the in-plane compressive properties are more critical for wind turbines while the out-of-plane compressive properties are more significant in the applications of automotive industry. Therefore, different properties or characteristics of sandwich panels need to be taken into account depending on the field of application (Donga 2011).

Donga (2011) studied the mechanical behavior of sandwich front bumper under static loading and improving the front bumper performance. Also, the composite sandwich beam Finite Element (FE) model was created and computationally tested under the three-point bending and its optimization applied by different orientations and the number of plies of the face sheet. In his study, sandwich section positively affected energy-absorbing behavior and provided to increasing of its crashworthiness. This sandwich structure with carbon/epoxy face sheet is more effective than a steel car bumper. Besides, Xiong et al. (2014) studied the mechanical properties and failure modes of carbon fiber composite egg and pyramidal honeycombs cores under in-plane compression. They investigated the failure of these composite sandwich panels subjected to in-plane compression via the analytical, experimental and numerical techniques. In the analytical part of the study, several failure modes as Euler or core shear macro-buckling, face wrinkling, face sheet crushing, core member crushing and face inter-cell buckling were observed and theoretical relationships for predicting the failure load associated with each mode were presented. The failure mechanism maps were constructed in order to predict the failure modes with different structural parameters. In the experimental part of the study, three different sets of specimens with egg and pyramidal honeycomb cores were manufactured to study the failure modes. Finite element simulations were carried out to predict the failure of Euler buckling. The

mechanical properties of pyramidal honeycomb sandwich columns are much better than that of the egg honeycomb sandwich column.

2.3.1 Failure modes in sandwich structures

Sandwich structures are heterogeneous materials and components of these materials can be selected depending on the design parameters. However, this heterogeneity causes formation of more complex failure mechanisms and results in more complex failure mechanisms than conventional structural elements such as steel, concrete, wood. The main failure modes in sandwich constructions are adhesive bonding failure, face sheet compressive failure, core shear failure, indentation failure and wrinkling. The most commonly observed failure modes were exhibited in Figure 2.4 and brief information is given below (Manshadi 2011).

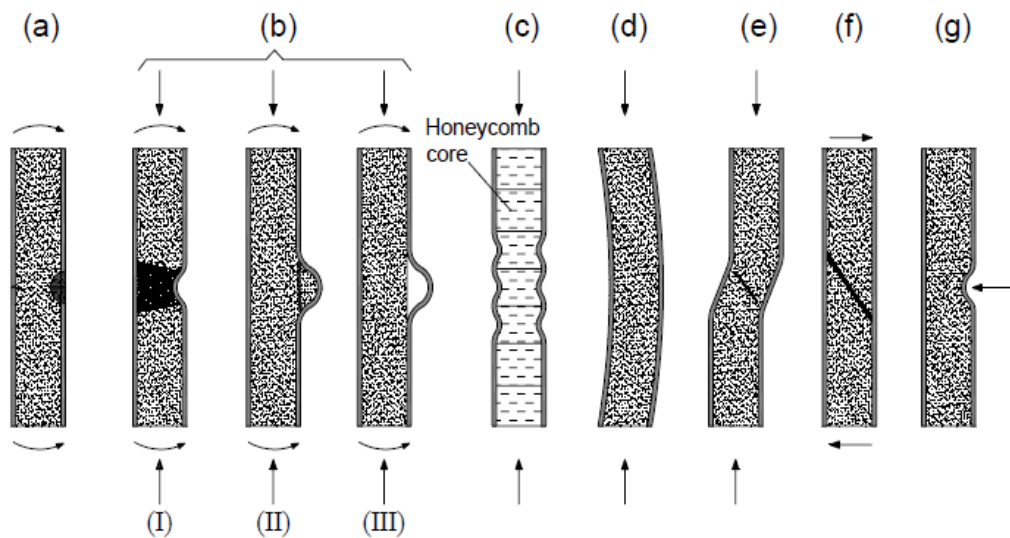


Figure 2.4. Typical failure modes of sandwich panels
(Source: Manshadi, 2011)

Tensile and compressive face sheet failure is shown in Figure 2.4(a) and this mode is observed when the face sheets are subjected to the maximum stress (at values of the yield or fracture strength). When local instability such as buckling and formation of shaped small waveform in the middle of the face sheet, face wrinkling can be observed as shown in Figure 2.4(b). This mode is very critical in lightweight sandwich

structures that have thin face sheets. The complete failure may occur in three failure types as seen in Figure 2.4(b); (I) crushing of the core and face sheet, (II) tensile rupture of the core and (III) tensile rupture of the core-to-face sheet bond. Better adhesion between face sheet and core can enhance tensile and compressive strengths. Figure 2.4(c) presents the face dimpling and this type of failure can be observed in sandwich structures that have discontinuous cores when the core has large cell size and face sheet is very thin. Both the cell walls that behave as edge supports and face sheet may buckle in the critical region. Figure 2.4(d) presents the global buckling mode and it is observed in sandwich structures that have stiff face sheets and thin cores. The global buckling includes overall bending of the composite wall coupled with transverse shear deformations. Shear crimping is one of the special forms of general instability and shown in Figure 2.4(e). It has very short buckle wavelength, because core has low transverse shear modulus. It occurs suddenly after the core shear failure or a shear failure in the core-to-face sheet bond. The core shear failure mode is observed when the core is subjected to greater stresses than its shear strength as shown in Figure 2.4(f). It should be noted that shear strength values of some core materials like honeycomb changes with the loading direction. Core indentation, shown in Figure 2.4(g) occurs when sandwich structures composed of thin skins bonded to the core having low compressive strength are not resistant to local loads that can easily indent them (Manshadi 2011).

In conclusion, these structures exhibit different failure modes when subjected to general bending, shear and in-plane loading. Generally, sandwich structures exhibit different properties depending on the properties of the core, the face sheets, the adhesive bonding the core to the skins, and geometric dimensions. Initiation, propagation, and interaction depend on the constituent material properties, geometry, and type of loading (Gdoutos and Daniel 2008). Properties of the core material also dramatically affect the initiation of failure in composite sandwich beams. Daniel (2009) studied the failure modes and criteria for their occurrence in composite sandwich columns and beams characterized by core materials including PVC foams and balsa wood. Sandwich specimens were subjected to bending moment, shear and axial loading and the observed failure modes compared with analytical predictions. The failure modes were; face sheet compressive failure, adhesive bond failure, indentation failure, core failure and facing wrinkling. The transition from one failure mode to another for varying loading or state

of stress was discussed. Experimental results were compared with analytical predictions.

Fan et al. (2013) studied the use of compliant skins to restrict debonding in carbon fiber reinforced lattice-core sandwich composites. Edgewise compression and three-point bending tests were carried out to deduce compression behavior and bending performances of these sandwich composites considering different skin thicknesses. Two typical failure mechanisms were observed; delamination and local buckling. Failure criteria were suggested and given consistent analytical predictions.

Hasseldine et al. (2015) studied the damage tolerance of sandwich composite panels that consist of 16-ply carbon/epoxy face sheets bonded to an aluminum honeycomb core under quasi-static indentation (QSI). Three different face sheet stacking sequences and three cores with varying density and thickness were studied to investigate the effects of ply angle change and core parameters on indentation damage and compression strength. The specimens were damaged in QSI to the barely visible indentation damage threshold by using spherical indenters of 25.4 or 76.2mm diameters. Damaged specimens were subjected to compression after indentation (CAI) to determine the compressive strength and resulting failure mode. CAI strength is compared to the undamaged strength obtained from edgewise-compression tests of specimens for the same geometry type. In these CAI experiments, three different failure modes including compressive fiber failure, delamination buckling and global instability were observed. As a result, indenter size has no effect on post-indentation compressive strength and/or particular failure mode for a given specimen geometry. The maximum damage resistance was observed on the specimens with a high core density and primary ply angle of 90° . Specimens with face sheets having the outer 0 plies closest to the center of the laminate were found to be the most damage tolerant.

V. Crupi et al. (2013) studied the static and low-velocity impact response of aluminum foam and aluminum honeycomb cored sandwiches. The effects of static and dynamic response and energy absorption capacity of these sandwiches were investigated and analyzed. The influence of indenter shape was examined by quasi-static indentation tests and resistance to indentation of honeycomb and aluminum foam sandwich panels were linked to the nose geometry, the cell diameter and the adhesion between the skin and core. The static bending tests were carried out at different support span distances on sandwich panels with the same nominal size. Different types of collapse modes were observed and they were explained by the simplified theoretical

models. The collapse mechanism as well as the face-core bonding and the cell size for foam and honeycomb panels affect the capacity of energy dissipation. They also carried out various low-velocity impact tests and observed different types of collapse mechanisms for two types aluminum sandwiches. The cell size dramatically affects observed collapse mode on honeycomb sandwiches because of buckling of the cells. On the other hand, collapse of the aluminum foam sandwiches was the foam crushing and their energy absorbing capacity was related to the foam quality. If the most cells of the metal foam are both similar sized and defect-free, it is said that the foam is in good quality. According to the energy balance model and model parameters, the impact response of the honeycomb and foam sandwiches was investigated using a theoretical approach. The use of these aluminum sandwich structures, based on rudiments that obtained from the experimental tests in weight reduction applications of the ships, can provide a sufficient structural strength under operating conditions.

S. Shi et al. (2014) designed and produced carbon fiber sandwiches which are composed of three different type cores, modified the interfacial mismatch by thin aramid-fiber tissue at the interface. Adding an orthogrid structure into the sandwich structure increases the stiffness of soft honeycomb despite of reducing the interfacial mismatch. The core then became an aluminum orthogrid structure filled with aluminum-honeycomb blocks. Three different sandwich structures, having carbon fiber face sheets and also interfacial aramid-fiber tissue reinforcement, are considered; (i) aluminum honeycomb core, (ii) aluminum-plate orthogrid core and (iii) aluminum plate orthogrid core filled by aluminum-honeycomb blocks. Three-point bending tests were applied to the sandwich structures. Although orthogrid core in sandwich structure caused a little weight increase, orthogrid structure improved the specific strength, critical load and energy absorption ability. Additionally, it was observed that the thin aramid fiber tissue significantly enhanced the delamination resistance of the interface region.

Amraei et al. (2013) studied the use of aluminum honeycomb (HC) as an energy absorber in high-speed train nose application. They designed a light-weight nose that has maximum energy absorbing, because train's frontal nose is the first damaged part at the frontal impact. The authors simulated the behavior of aluminum HC sandwich panel with both shell and solid elements under dynamic crush loads. Finite element simulations were performed by using LS-DYNA. They also investigated the effects of the nose of various HC thicknesses and change the length of high-speed train nose on

crashworthiness characteristics and weight. They proposed the optimum thickness and compared the amount of absorbed energy. As a result, energy absorption increased with increasing the length of nose and maximum amount of energy absorption of the nose with 4m length is found to be 1621.80 kJ. Also, it was note-worthy that the maximum forces for different lengths reached to a constant value. It was observed that for all thicknesses the amount of energy absorption has been increased about 35%.

J. U. Cho et al. (2013) studied the behavior of composites with porous cores after impact. These sandwich composites with aluminum honeycomb cores were subjected to three different impact energies; 50, 70 and 100 J. The striker penetrated the upper face sheet and broke the material in every case when the maximum force reached to 4.5 kN. The maximum force was observed at 4.0, 3.5, and 3.0 ms for impact energies of 50, 70, and 100 J, respectively, indicating that the maximum force occurred sooner when the impact energy was greater. They showed that the penetration of aluminum honeycomb core sandwiches was related to the impact energy. Below 50 J, the striker did not penetrate the lower face sheet, and the honeycomb core sandwich was stable. According to this result, the maximum load occurred when the striker penetrated the upper face sheet. As the striker penetrated the composite, the load gradually decreased after the striker penetrated the core, remained constant, and then increased rapidly after the striker came in contact with the lower face sheet. Simulation results showed good agreement with the experimental ones. The authors concluded that these experimental results could be applied to actual conditions in the field and the stability of aluminum honeycomb core sandwich composite structures could be predicted from these experimental results.

Mozafari et al. (2015) studied the in-plane and crushing properties of aluminum honeycomb core and polyurethane foam with different densities 65, 90 and 145 kg/m³. They manufactured foam filled honeycomb panels, and carried out experimental quasi-static compression tests. Additionally, the authors made finite element analyses for three different honeycomb cores that were filled three types of polyurethane foams. The effects of foam filling of aluminum honeycomb core on its in-plane mechanical properties such as mean crushing strength, absorbed energy, and specific absorbed energy were investigated both experimentally and numerically. The results showed that the foam filling of honeycomb core could increase the in-plane crushing strength and specific absorbed energy up to 208 and 20 times, respectively.

Singh et al. (2014) studied the damage resistance of composite sandwich structures that consist of carbon/epoxy face sheets that 8 and 16 ply quasi-isotropic and two aluminum honeycomb cores that have different densities and thicknesses. Four face sheets have different stacking sequences were utilized for each thickness. Additionally, the face sheet thickness and other parameters that have different core thickness, core density, face sheet layup, and indenter diameter. The external damage was measured quasi-statically using spherical steel indentors with different sizes and the damage metrics and the effect of these parameters on the extent of damage is evaluated considering the dent depth, dent diameter, and planar area of delamination. If the dent depth or diameter is considered as the damage metric, specimens having higher density core are always found to be the most damage resistant. When planar area of delamination is considered, the eight ply configuration comprised of a lower density core and face sheets are found to be the most damage resistant. 16-ply specimens are found to be the least damage resistant when this criterion is considered. In addition, 16-ply configuration with an angle of $\pm 45^\circ$ and a high density core provides the best delamination resistance.

Chun Lu et al. (2015) investigated mechanical performance and stress distribution of the composite honeycomb sandwich structure subjected to bending load. Firstly, carbon fiber/epoxy honeycomb was prepared and composite plates were manufactured by compression molding technique. Then, wave beams were adhesively bonded together and composite sandwich structure was prepared by gluing the core and composite face sheets (top plate and bottom plate) together. Three point bending performance of the composites was analyzed using finite element analysis (FEA). Stress concentration is located at the loading zone and supporting zone. When the load is increased to 7200 N, the cracks occur that cause interfacial debonding on the interface between honeycomb and composite panel. If the load is increased to 6800 N, crushing of the composite honeycomb sandwich is observed, as verified with FEA results. Carbon fiber/epoxy honeycomb sandwich was compared with traditional aluminum and nomex honeycomb sandwich and it was observed that carbon fiber/epoxy honeycomb sandwich has higher bending strength as well as more density. The highest stress distribution was on top-plate and the failure mechanism of composite honeycomb structure, cracking or debonding between surface plate and honeycomb structure was observed on top-plate.

A.S.M. Ashab et al. (2016) studied the mechanical behavior of the aluminum hexagonal honeycombs under combined compression-shear loads experimentally. They carried out the quasi-static and dynamic tests at five different loading velocities and by using specially designed fixtures in order to apply combined compression-shear loads to the honeycombs at various angles of 15°, 30° and 45° respectively. Three types of aluminum honeycombs with different cell sizes and wall thicknesses were crushed in two different plane orientations, namely TL and TW. The crushing force, deformation, plateau stress and energy absorption of aluminum honeycombs were determined. An empirical formula was derived to explain the relationship between loading angle and plateau stress. In the experiments, the honeycomb cell walls buckled and shearing occurred through rotation of the cell walls. Also, in the plateau region, the crushing force remained unchanged for a loading angle of 15°; the force decreased slightly for a loading angle of 30°; and the force decreased significantly at a loading angle of 45°. For the same loading velocity and loading angle, the plateau force was found to be slightly higher in the TW plane than in the TL plane.

Russell et al. (2011) investigated the behavior of quasi-static three-point bending of carbon fiber sandwich beams and failure modes of the beams. Sandwich beams were manufactured from carbon fiber composite sheets and a square honeycomb core. Firstly, they manufactured and tested sandwich beams with face sheets and square honeycomb cores each made from a carbon fiber composite. The beams were loaded in three-point bending, in both the simply supported and clamped conditions. Analytical calculations were made for four collapse mechanisms. These were; (i) face micro-buckling, (ii) core shear, (iii) core indentation and (iv) face wrinkling. Selected geometries of sandwich beams were tested to illustrate these collapse modes, good agreement was found between analytic predictions and measurements of the failure load. Finite element (FE) simulations of the three-point bending responses of these beams were also carried out by constructing a FE model by laying up unidirectional plies in appropriate orientations. The initiation and growth of damage in the laminates were also considered in the FE calculations. The FE model was good at predicting the measured load versus displacement response and the failure sequence in each of the composite beams.

Coskun and Turkmen (2012) studied the bending fatigue behavior of laminated sandwich beams under flexural cycling loadings. Sandwich beams were made of carbon/epoxy face sheets and aramid honeycomb core. They were manufactured by wet hand lay-up technique. Flexural fatigue tests were carried out at constant loading

frequencies of 7 Hz and 10 Hz. For the purpose of two cylindrical loading noses, the free edge was loaded while one end of the material specimens was clamped. Fatigue tests were applied with two different displacement amplitudes; ± 10 mm and ± 15 mm. It was observed that number of cycles and maximum load, was the initial load at the beginning of the flexural test, directly affected by changing of maximum load. The authors investigated the bending stiffness, mechanical properties and free vibration frequencies of the sandwich beam. The flexural and vibration identification tests were carried out by using a vibration analyzer, a hammer and an accelerometer to measure the bending stiffness and free vibration frequencies of the sandwich beams before and after fatigue tests under clamped condition. The bending stiffness and free vibration frequencies tests were compared to deduce the effect of repeated loadings on the mechanical performance of the laminated sandwich beams. It was observed that the fatigue behavior of the sandwich composites relied on the different damage mechanisms such as fiber bridging, matrix cracking, interfacial debonding between core and skin, and shear cracks in the core.

2.4. Constituents of Composite Sandwich Structures

Sandwich composites are primarily composed of two components, namely skin and core. If an adhesive is used to bind skins with the core, adhesive layer can also be considered as an additional component in the structure. The thickness of the adhesive layer is generally negligible because it is much smaller than the thickness of skins or the core (Njuguna 2016). The overall performance of composite sandwich structure depends on the mechanical properties of its constituent materials, a detailed knowledge on the behavior of the skin and the core is a fundamental requirement for the effective utilization of fiber composite sandwich structure (Manalo et al. 2012). The constituents should be also selected by considering the application area and working environment. Both core and face-sheet types vary with respect to the design requirements and the manufacturing of sandwiches depend on these components (Basturk 2011).

2.4.1. Face sheet Materials

Although metal, wood, plastic, FRP composites or any other materials can be used in a sandwich structure as a face sheet material, commonly, aluminum, glass, carbon and aramid fibers are usually preferred for structural applications, depending on the required strength, stiffness, corrosion resistance and allowable budget. Primarily, face sheet should be selected by considering the application area and working environment (Basturk 2011, Hollaway and Head 2001).

2.4.1.1. Composite Face sheets

The average thickness of the composite face sheets varies between 0, 15 mm and 5 mm in compliance with the design specifications. Flexibility in design is an advantage to reduce the overall weight of the structure so that one can eliminate redundant materials from uncritical areas. Composite materials have physical and chemical stability against the exposed environmental conditions. Also, proper matrix and reinforcement materials must be selected for the application fields of the structure.

In composites, fibers carry the applied load on the composite structure and they provide strength, stiffness, thermal stability and other structural properties for face sheets. The main role of matrix material is to bind together the fibers. The matrix material also transfers the load to the fibers. Also it provides good resistance to the most environmental effects like moisture, humidity as well as chemical attack and mechanical damage (Donga 2011).

2.4.1.1.1. Face sheet Matrix Materials

Face sheet matrix resin is the continuous phase that performs two major roles. One is to protect the reinforcement from adverse environmental effects and abrasion. The other is to provide uniform load distribution to the fiber. In order to transfer the load uniformly between the two distinct phases, the adhesion between the matrix resin and fiber is very crucial. The mechanical stability and capacity of the polymer matrix based composite laminates is strongly related to bonding between their components and the mechanical performance of the matrix (Pilato and Michno 2013, Strong 1989).

Matrix resins sufficiently must have high strength and shear modulus that can hinder the buckling of fiber under compression load. Also the absorbing energy and decreasing stress concentrations should be provided by the ductility of the matrix to maximize damage tolerance and long term durability. In addition, hot/wet performance of the resin is very critical. Matrix resin is sensitive to water and hostile environment conditions. A little increase in polymer may be observed because of the continued cycling from dry to wet environments.

The volume changes like swelling and shrinkage of resin matrix under these conditions may cause micro-cracking. The combined effects of creep, fatigue, moisture, and temperature cause the failure of the composite structure (Pilato and Michno 2013). Only, temperature and time can affect the viscoelastic properties of materials. Moisture influences the polymeric matrix as a plasticizer, reducing the glass transition temperature. Besides, moisture changes the time-dependent mechanical response. Therefore, designers must be very careful when they need to select the composite material. Generally, two types resins used. These are thermosetting and thermoplastic resins (Strong 2008).

The most common thermosetting resins are epoxy, polyester and vinyl ester resins and these resins are irreversible polymer materials after their curing completed as well as in the liquid form. For example, chemical reaction is necessary for curing of the epoxy resins while the curing of cyanate ester resins may be effected by heat and vinyl ester resins are cured by irradiation such as; an infrared, ultraviolet light, or electron beam. Once cured, even if the material is reheated, it cannot be melted back to its original liquid form. Thermosetting resins are easily processed and laminated. Despite of the fact that they are relatively more brittle, they are generally inexpensive, stronger and have better properties at higher temperatures compared to thermoplastics and they are formed without the need heat or pressure (Soo-Jin Park 2014).

Epoxies are the most common thermosetting resins and they are preferred for advanced composites and various demanding applications as matrix due to their superior properties: excellent adhesion, good corrosion resistance, high strength, processing versatility and lower shrinkage than polyester resin. Also, toxic gases like styrene do not released into the atmosphere during the manufacturing and curing process. Uncured epoxies also emit some gases but these are not as harmful as styrene. The range of operating temperatures of epoxy resins is between 60⁰C-140⁰C. This is

higher than polyesters but lower than that of polyimides. On the other hand, epoxies have higher cost and viscosity than polyesters (V. Hoa 2009).

Polyester resins have many advantages; they are very easy to use, the most economical resin systems and they have also good chemical resistance. Most polyesters are prevented to air and will not cure when exposed to air. Typically, paraffin is added to the resin formulation, which has the effect of sealing the surface during the cure process. However, the wax film on the surface presents a problem for secondary bonding or finishing and must be physically removed. Non-air inhibited resins do not present this problem and are therefore, more widely accepted in the marine industry (Associates 1999).

Thermoplastics are one or two dimensional molecular structures; they are not cross-linked unlike thermosets. Their stiffness and strength properties come from their inherent properties of the monomer units and high molecular weight. The thermoplastics generally soften at high temperatures and are formed in a mold. The main thermoplastics are polyethylene, polystyrene, polypropylene, polyamides and nylon. They have generally limited use in the marine industry such as, small boats and recreational items. But, in filament winding processing, they are not more preferable than thermosets with regard to enhance damage tolerance and thick sections of products (Associates 1999).

2.4.1.1.2. Face sheet Reinforcement Materials

Fibers are dominant in mechanical properties of composites. Because fibers carry all loads due to the fact that external stresses are transmitted to the fibers by matrix. Also, matrix protects the fibers against the environmental effects. Thereby, fibers should be selected depending on the desired properties in composite structures. Therefore, a designer should prefer to available fiber type considering the requirements. As a reinforcement, three type fiber are commonly used in most engineering applications. These are carbon, glass and aramid (Strong 1989 and Kessel 2004).

Carbon or graphite fiber is one of the most common fibers and it is used extensively in the aerospace industry. It consists of small crystallites of graphite and generally about 8 μm in diameter and has a lot of advantages such as; high specific strength and modulus, high fatigue strength, low density, high stiffness and low

coefficient of thermal expansion as well as its drawbacks such as; high cost, low impact resistance, and high electrical conductivity. Carbon fibers present the high tensile strength and modulus characteristics even at elevated temperatures (Kessler 2004 and Kaw 2006). Also carbon fibers are capable of using with all type matrices such as; polymer, ceramics and metals due to the fact that these fibers can maintain its characteristics at excessive temperature and pressure. Additionally, different composite processing techniques are needed to carry out (Mortensen 2007).

Glass fibers are the most common fiber using in non-aerospace applications due to the fact that they have the advantages of the high strength, high chemical resistance, low cost and good insulating properties, moderate strength and weight. Although the main chemical constituent of the glass fiber is silica (SiO_2), glass fiber includes other oxides, such as B_2O_3 and Al_2O_3 . The ratio of these added components provides to modify the network structure of silica and to obtain to fiber glasses which has different structure and properties. Three are three main types of glass fiber are C-glass, E-glass and S-glass. E glass (Electrical) is generally utilized for electrical applications because of the fact that it is an excellent electrical insulator. It usually chooses as a structural reinforcement owing to its sufficient mechanical properties and lower costs. S-glass (Strength) has the highest specific strength and stiffness but is significantly more expensive than E-glass. C-glass (corrosion) is used in acidic environment conditions, because it is advantageous in resisting to chemical corrosion, but C-glass has lower strength (Schwartz 1997). The manufacturing of Glass fibers is provided by the mechanical drawing of the flow of the melted raw materials as well as the gravity. There are different the controlling parameters in order to control the diameter of the glass. These are the head level of the melted glass in the tank, the viscosity of the glass and the diameter of the holes that the raw material is drawn. Generally, the diameter of the E-glass ranges from 8 to 15 μm (Barbero 2011).

Aramid fibers were firstly released by Du Pont in the early 1970 and trading name of them is Kevlar. They are organic aromatic compounds and comprises of carbon, oxygen, hydrogen and nitrogen. These fibers showing anisotropic property have various advantages such as; low cost, high tensile strength, and high impact resistance as well as having the lower density than other fiber reinforcements. The major disadvantages of them are such as; low compressive strengths, degradation in sunlight and difficulty in machining and cutting.

There are two main types of aramid fibers, Kevlar 29 and Kevlar 49. In spite of the fact that both of specific strengths of Kevlar fiber types are similar, Kevlar 49 has a higher specific stiffness. Kevlar 29 is mainly used in bullet proof vests, ropes, and cables. Kevlar 49 is preferred high performance applications in the aircraft industry. The manufacturing of the fibers is performed with preparing a solution of proprietary polymers and strong acids. Then, this solution is extruded into hot cylinders at 200°C, washed and dried on spools. Lastly, for increasing rigidity and strength of the fibers, stretching and drawing operations are applied (Kaw 2006 and Schwartz 1997).

2.4.1.1.3. Manufacturing Methods of Polymer Matrix Composite (PMC's)

Manufacturing process changes depending on types of matrix and fibers. In order to be formed the part and curing the matrix as well as the cost effectiveness of the process, the temperature is required. Usually, the primary consideration in the design of a composite structure is the manufacturing process, because adequacy, cost, production volume and production rate of a manufacturing process are important for producing the required structure type. Understanding the advantages, limitations, costs, production rates and volumes and typical uses of various manufacturing processes is required for designers due to the fact that each manufacturing process possesses certain limitations on the structural design. The material and structure are simultaneously designed in the design of a composite structure. Additionally, right choice of the material provides advantages to designer in terms of high mechanical performance and freedom in design. As a result, there are a lot of manufacturing processes and these are hand lay-up, prepreg layup, bag molding, autoclave processing, compression molding, resin transfer molding (RTM), vacuum assisted resin transfer molding (VARTM), pultrusion, and filament winding.

Processing of polymer matrix composites involves the following unit operations (Barbero 2010):

1. Fiber placement along the required orientations;
2. Impregnation of the fibers with the resin;

3. Consolidation of the impregnated fibers to remove excess resin, air, and volatile substances;
4. Cure or solidification of the polymer;
5. Extraction from the mold; and
6. Finishing operations, such as trimming.

2.4.1.1.3.1. Hand Lay-up

The hand lay-up technique is also called as wet lay-up and this technique is the simplest and most common manufacturing process. The dry reinforcements manually are placed into the mold and they are successively wetted by resin. Then, in order to facilitate uniform resin distribution and removal of air pockets, the wet composite is rolled by hand rollers. The stacking process of fabric materials and resin is repeated until the required thickness is obtained. Then, layered structure is cured. Although this method is appropriate for production in low volume, It has disadvantages such as; low quality control and inconsistency in properties of various parts of the finished product as well as the fact that high emission of volatiles such as styrene. In addition, the hand lay-up process can be classified into four basic steps: mold preparation, gel coating, lay-up, and curing (Barbero 2010).

2.4.1.1.3.2. Resin Transfer Molding

Resin transfer molding (RTM) has been accepted as a composite manufacturing process since the mid-1980s due to demand of the automotive industry that needs high volume production net shape structural parts. It was possible to form net shape structures at high volumes by injection and compression molding of discontinuous fibers, but desired performance could not be achieved. Thus, continuous fibers were placed a net shaped mold and then the resin was injected under high pressure to cover the empty spaces between the fibers. There are micron sized spaces among the fibers, accordingly low viscosity resins should be used due to the resistance to flow. Although thermoset resins were chosen for this process, there has been some recent activity in bringing to market thermoplastic resins with low viscosity (Advani and Hsiao 2012).

2.4.1.1.3.3. Vacuum Assisted Resin Transfer Molding (VARTM)

VARTM is known as the vacuum infusion process and commonly used in composite production. When the VARTM compared with RTM, it is seen to have some differences. In VARTM, resin is slowly filled to mold under lower pressure and resin flow into the mold depending on the pressure can be changeable due to the flexible top surface. Therefore, the fiber volume fraction will be lower than expected if the necessary measures are not taken. Also, the molds used in VIP do not need to be metal and this process has some advantages. It has lower cost than RTM with regard to materials, molds and equipments and environmental hazards can be reduced due to having closed mold. Although this process can provide producing of many parts inexpensively due to the low pressures that allow to use of thin molds. Also, support mechanisms are frequently used in this mold. Products such as tennis racquets, racquetball hardware, bicycle parts and component housings for snowmobiles and watercraft, can be produce by the VIP process (Strong 2008).

In this process, only a sided mold suitable for intended structural geometry is utilized and dry fabrics are stacked on the mold. The mold is then covered with a vacuum bag and a vacuum is applied to remove the air from the mold. After this operation completed, resin is transferred from a reservoir under atmospheric pressure. Vacuum be applied until ensuring complete mold filling. Then, resin is cured under suitable conditions (Advani and Hsiao 2012).

2.4.2. Core Materials

The core material is another main component of composite sandwich structures. In a sandwich structure, tensile and compressive loads cannot be carried by the core but, the core resists the transverse shear loads and increases the rigidity of whole structure (Mallick 1997). The face sheets are generally identical in material and thickness. The type of sandwich constructions is one of the most important factors determining the configuration of the core. The effectiveness of the sandwich structure can be preserved, if the core must be as much stronger as it can resist compressive or crushing load placed on the panel. If collapses occur in the core, the mechanical stiffness cannot be mentioned. Core densities ranges from 16 kg/m^3 to 900 kg/m^3 (Donga 2011). The core

materials are generally divided into four types. These are foam or solid core, web core, honeycomb core, and corrugated or truss core (Vinson 1999).

Foam or solid cores that are relatively inexpensive consist of balsa wood and an almost infinite selection of foam/plastic materials, with a wide variety of densities and shear moduli. Balsa is one of the most popular light woods because of its good strength and having low density (approximately 128 kg/m^3). Due to the fact that it perfectly is distributed and has low cost it is prefer in many industrial, commercial and marine applications (Lee 1992). The second type of core material frequently used in adhesively bonded structure is foam core. Although foam cores have worse mechanical properties when compared to honeycomb core, they are utilized widely in such commercial applications as boat building and light aircraft construction. The average core density can vary between values of 32 and 640 kg/m^3 . The Polystyrene, Polyvinyl chloride (PVC), Polyurethane and Polymethylmethacrylimides foams are most commonly preferred structural foams. In structural applications, completely understanding the chemical, physical, and mechanical properties of any foam is very considerable, particularly in terms of solvent and moisture resistance and long-term durability. Depending on their chemistry, operating temperature of the foam core materials is in the temperature ranging between $70 \text{ }^\circ\text{C}$ and $200 \text{ }^\circ\text{C}$.

Polystyrene cores are lightweight, low cost, and easy to sand, but they have low mechanical properties. Therefore, they do not prefer in structural applications. Although the styrene will dissolve the core in the resin, they cannot be utilized with polyester resins.

Polyurethane foams can be thermoplastic or thermoset due to degrees of closed cells. They can be found in finished blocks form or as formulations which can be mixed and foamed in place. Moderate mechanical properties of polyurethane foams lead to skin delamination.

Polyvinyl chloride (PVC) foams are among the most widely used core materials for sandwich structures. While crosslinked PVC foams have thermoset properties which have higher mechanical properties and higher resistance to solvents and temperature, uncrosslinked ones behave as thermoplastics which are tougher, easier to thermoform and more damage resistant. Crosslinked foams are more brittle and more difficult to

thermoform than uncrosslinked foams. Dimensional stability of PVC foams are enhanced by a heat stabilization treatment.

Styrene acrylonitrile foams can also be preferred, while their mechanical properties are similar to crosslinked PVCs and their toughness and elongations are similar to uncrosslinked PVCs. Ability of scribing of grooves patterns in the surfaces of foams is useful for resin transfer molding.

Polymethylmethacrylimides, which have excellent mechanical properties and good solvent and heat resistance, are lightly crosslinked closed-cell foams. They can be thermoformed to contours and are capable of withstanding autoclave curing with prepregs. These foams are expensive and are usually reserved for high-performance aerospace applications (Campbell 2010).

2.4.2.1 Honeycomb Structures

Honeycomb is utilized mostly for structural applications in the aerospace industry due to its properties such as; fire retardant, flexible, lightweight, and has good impact resistance. It also offers the best strength to weight ratio of the core materials. Honeycomb structures can be manufactured from different materials, depending on the field of application and required characteristics. For example, while a paper honeycomb is used for low strength and stiffness for low load applications, metal or composite honeycombs that have high strength and stiffness are preferred in high performance applications. The strength of sandwich panels are affected by the size of the panel, used facing material and the number or density of the cells within it (Vinson 1999).

In addition, honeycomb structures are geometrically classified into three main categories as seen at Figure 2.5. These are square honeycombs, hexagonal honeycombs, and triangular honeycombs. Triangular honeycombs are difficult to make, and not widely used. A number of methods have been devised over the years for fabricating square and hexagonal honeycomb structures, and this includes a slotting and brazing approach, slotting and adhesive bonding, and by stacking of corrugated layers (George 2014).

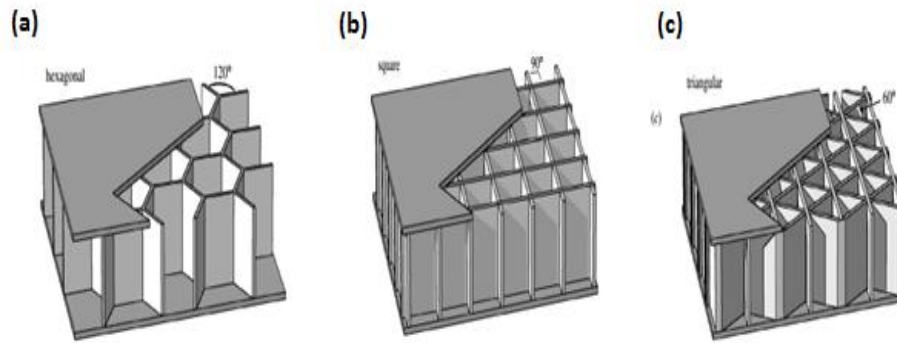


Figure 2. 5. Examples of the three forms of honeycomb shown as core structures in sandwich panels: (a) hexagonal honeycomb, (b) square honeycomb and (c) triangular honeycomb (Source: Waldey 2006).

2.4.2.1.1. Manufacturing of the Honeycomb Core Structures

Although several approaches to make metallic honeycomb structures have been developed, two main techniques are used in manufacturing of honeycomb materials. These are the expansion process and the corrugation process.

Expansion manufacturing process generally preferred to fabricate of low density hexagonal honeycombs. In this process, firstly, panels that cut from thin metal sheets are bent as intended and strip bonded. Thus, honeycomb before expansion or hobe block is obtained. In order to generate hexagonal structure, this hobe block should be cut and stretched perpendicular to thickness. In expansion process, inter-sheet bond strengths should be high as sufficient to enable sheet stretching. Low-density honeycombs with very thin webs that have desired bond strengths can be manufactured using the processes such as; diffusion bonding, modern adhesives and laser welding. But the web (sheet) thickness increases with increasing cell size ratio, so it means increasing the relative density. Eventually, the force required to stretch the metal sheets approaches the inter-sheet bond fracture strength. Other manufacturing methods should be used for manufacturing of the higher relative density hexagonal honeycombs (Wadley 2006).

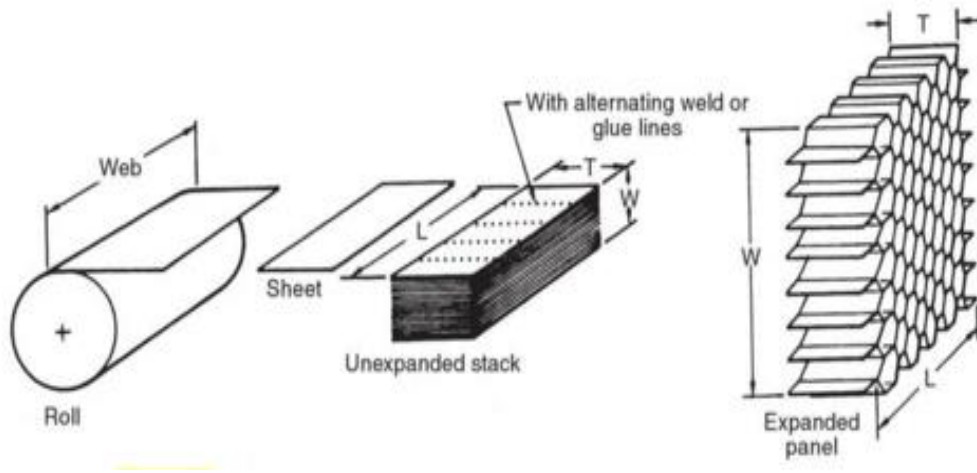


Figure 2.6. Honeycomb manufacture by the expansion process

(Source: Erik Lokensgard, 2008)

The corrugation process, another honeycomb manufacturing technique, is as seen in Figure 2.7. In this approach, firstly a metal sheet is formed as corrugated, and then stacked. The sheets are bonded by welding or adhesive and obtained cores are sliced according to the intended thicknesses. In addition, the making honeycombs from less ductile materials rudiment this slotted sheet process is more suitable because of the fact that metal bending is not required. Moreover, it is in principle possible that brittle honeycombs like composite or ceramic are produced using this approach (Wadley, 2006).

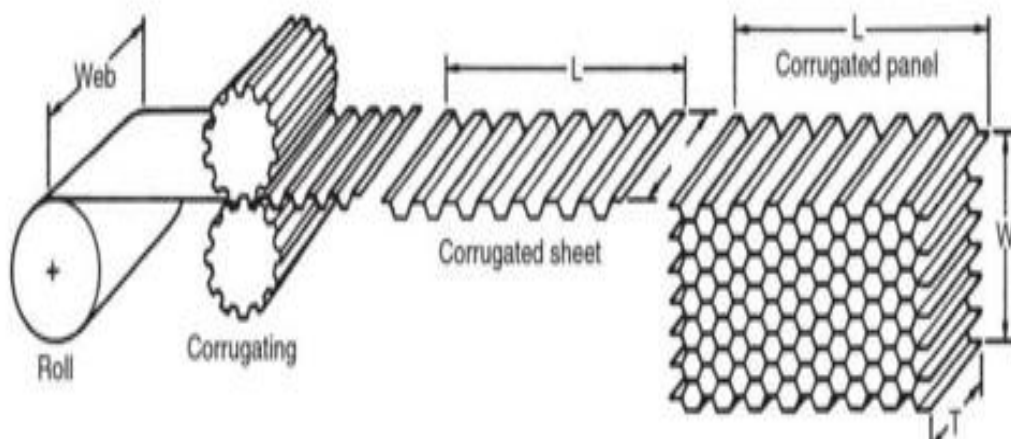


Figure 2.7. Honeycomb manufacture by the corrugation process

(Source: Erik Lokensgard, 2008)

CHAPTER 3

EXPERIMENTAL

3.1. Materials

Unidirectional (UD) carbon fiber based fabrics (MetaxTM CWUD 500A) were used as the reinforcement constituent of the composite face sheets. Epoxy resin (MomentiveTM MGS L160) with hardener (MomentiveTM MGS H160) was used as the matrix material. Aluminum honeycomb core materials with hexagonal cell configuration (with cell size of 10 mm) were provided by 6Gen Panel Aerospace Shipbuilding Panel Industry of Turkey. Three different core thicknesses; 6, 21 and 46 mm were used for the manufacturing of the composite sandwich panels. Figure 3.1 is an example illustration of the honeycomb core material.

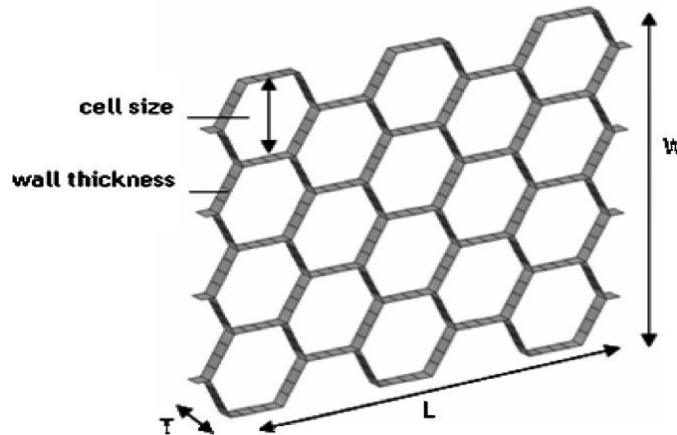


Figure 3.1. Nomenclature of the hexagonal honeycomb core material
(Source: Aktay et al. 2008)

3.2. Manufacturing of Composite Sandwich Panels

Composite sandwich panels consisting of carbon fiber/epoxy face sheets and aluminum honeycomb core materials with various thicknesses were manufactured. At the first stage, composite face sheets were produced by vacuum infusion technique. Dry carbon fabrics were placed on a smooth infusion table with a stacking sequence of

[0/90]_s. The infusion part was prepared by using infusion materials such as vacuum bag, distribution media, etc. The resin was allowed to flow through the entire fabric network, while the part was kept under vacuum. After completion of the infusion, the parts were allowed to cure at room temperature followed by post-curing for 12 hours at 80°C. Test specimens were cut into desired dimensions by water-cooled diamond saw according to relevant ASTM standards. In order to improve bonding at face sheet/core interface, one surface of the composite face sheets was sanded with 80-grit sandpaper and cleaned by acetone. Face sheets and core materials were bonded together by a polyurethane (PU) based adhesive. The adhesive was applied onto sanded surface of composite facesheets and they were sandwiched together with aluminum cores. The sandwiched specimens were laminated at room temperature under the pressure of 10 kPa. Curing was applied in an oven at 60°C for 35 minutes and post-curing was performed at room temperature for seven days for completion of curing of adhesive material. Flow chart of composite sandwich fabrication is given in Figure 3.2

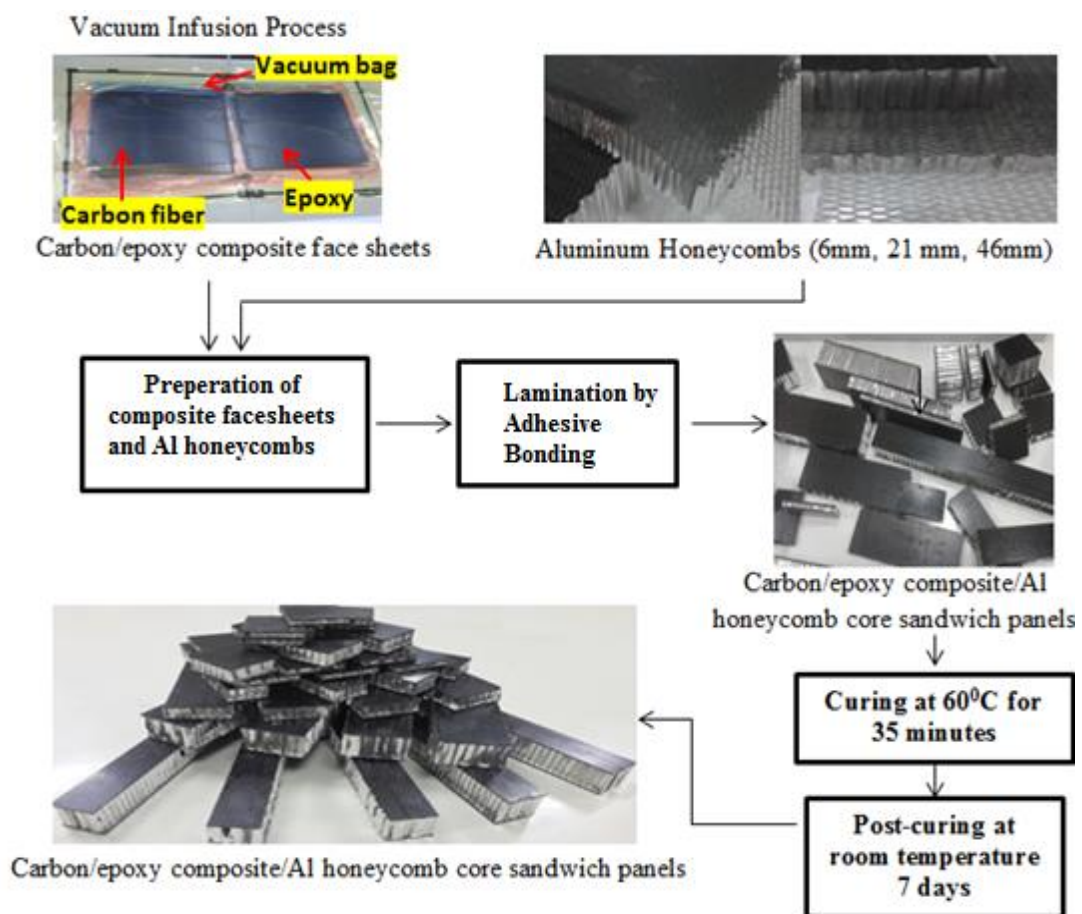


Figure 3.2. Flow chart of composite sandwich structure manufacturing

3.3. Characterization Techniques

3.3.1. Honeycomb Core Material

3.3.1.1. Optical Microscopy

The cells wall thicknesses of the Al honeycomb core materials were measured by using Nikon™ optical microscope.

3.3.1.2. Flatwise Compression Test of Al Honeycomb Materials

The flatwise compressive strength and modulus of the Al honeycomb core materials were determined according to ASTM C365M-11a. Flatwise compression test specimens were cut into square shape with 70 mm edge for each core thickness using a cutter. The tests were performed by using a Schimadzu™ testing machine at a crosshead speed of 0.5 mm/min. At least five specimens for each thickness were tested. Figure 3.3 shows a flatwise compression test specimen under loading.

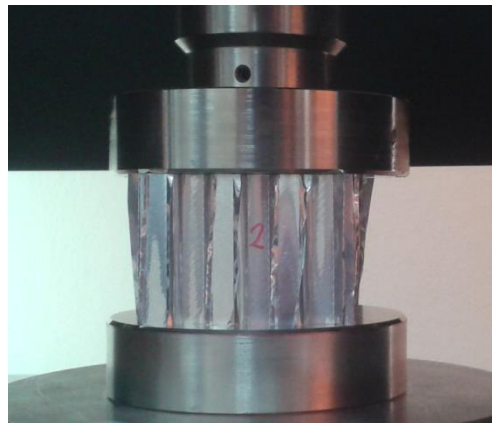


Figure 3.3. Flatwise compression test specimen (Al honeycomb core) under loading

The flatwise compressive strength (σ) values were calculated using the following equation;

$$\sigma = \frac{P}{A} \quad (3.1)$$

In the equation, P is the ultimate load and A is the cross-sectional area of the specimen. Core compressive modulus (E) values were calculated by using the following equation;

$$E = \frac{Sc}{A} \quad (3.2)$$

Here, S is the slope of the initial linear portion of load-deflection curve ($\Delta P/\Delta u$) and c is the core thickness.

3.3.2. Composite Face Sheet Material

3.3.2.1. Determining Fiber Volume Fraction

Experimental measurements of the fiber content for carbon fiber composite were conducted by the density method. The fiber volume fraction was obtained by this method that can give a quick and good estimate. The densities of carbon fiber and resin were taken as 1.70 g/cm^3 and 1.16 g/cm^3 , respectively. The fiber volume fraction of the carbon fiber specimens was calculated by measuring the density of the composite in air and in distilled water. To determine the V_f , five specimens were cut from composite plate; each sample was dried and weighed in air. Each sample was then immersed in water and weighed in distilled water. The density of the composite materials was calculated by Archimedes' Principle using the following equation:

$$\rho_c = W_{air} \rho_{water} / (W_{air} - W_{water}) \quad (3.3)$$

In this equation; ρ_c is density of composite, ρ_{water} is density of distilled water, W_{air} is the weight of sample in air and W_{water} is the weight of sample in distilled water.

The fiber volume fraction of composite plate was measured by using the rule of mixtures as given below:

$$V_f = (\rho_c - \rho_{resin}) / (\rho_{fiber} - \rho_{resin}) \quad (3.4)$$

3.3.2.2. Tensile Test

ASTM D 3039M-14 was used to determine the tensile strength and modulus of the composite face sheets. Test specimens were sectioned from the composite panels with of 25 mm in width, of 2.5 mm in thickness and 250 mm in length. At least five specimens were prepared using a diamond saw. The specimens were tested using Shimadzu™ universal test machine (AG-IC 100 kN) at a cross head speed of 2 mm/min (Figure 3.4).



Figure 3.4. Tensile test specimen (composite face sheet) during the test

The tensile strength (σ) values were calculated by the following equation;

$$\sigma = \frac{F}{A} \quad (3.5)$$

where F is the ultimate load, and A is the cross sectional area of the specimen. Elastic modulus was obtained from the initial slope of stress (σ) - strain (ϵ) curves based on the equation below;

$$E = \frac{\sigma}{\epsilon} \quad (3.6)$$

3.3.2.3. Compression Test

ASTM D 6941-14 was used to measure the compressive strength and modulus of the composite face sheet panels. Compression test specimens with 13 mm in width

and 140 mm in length were cut from face sheet panels using a diamond saw. These specimens were tested using the mechanical test machine at a crosshead speed of 1.3 mm/min. At least five specimens were tested using the universal test machine (UTM).

3.3.2.4. Flexural Test

The flexural test method was used to determine the flexural strength and modulus of the composites according to ASTM D 790-15. Test specimens with 13 mm in width, 2.5 mm in height and 100 mm in length were sectioned from the face sheet panels using a diamond saw. Specimens were tested by using a 3-point bending apparatus with a span to thickness ratio of 32. Figure 3.5 shows the flexural test specimen under loading. At least five specimens from composite face sheets were tested using the universal test machine at a crosshead speed of 4.37 mm/min. During the test, force vs. deflection of the beam was recorded.

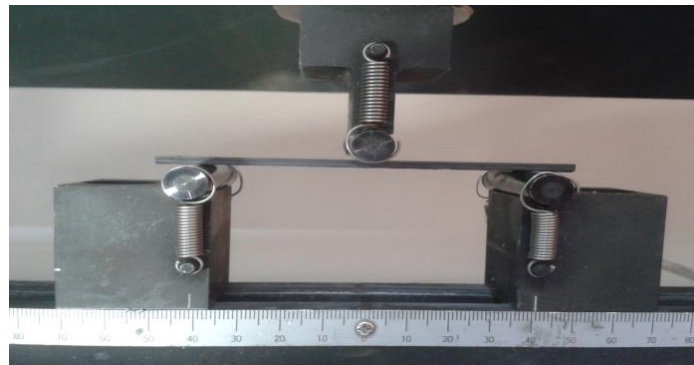


Figure 3.5. Flexural test specimen (composite face sheet) under loading.

The flexural strength, S , values were calculated from the equation below;

$$S = \frac{3PL}{2bd^2} \quad (3.7)$$

where P is the applied load at the deflection point, L is the span length; d and b are thickness and width of the specimen, respectively. The maximum strain in the outer fibers occurs at midspan and calculated with the equation below;

$$r = \frac{6Dd}{L^2} \quad (3.8)$$

where r is the maximum strain in the outer fibers, D is the deflection. The flexural modulus values, E_b were calculated with the equation;

$$E_b = \frac{L^3 m}{4bd^3} \quad (3.9)$$

where m is the slope of the tangent to the initial straight line portion of the load deflection curve.

3.3.2.5. Interlaminar Shear Test

The interlaminar shear strength (ILSS) of the composite specimens was determined performing short beam shear (SBS) tests according to ASTM D2344-13. The SBS specimens 18 mm in length, 3 mm in height and 6 mm in width were cut from the composite facesheets. The length to thickness ratio and span to thickness ratio were 6 and 4, respectively. The crosshead speed was 1 mm/min and five specimens were tested using the universal test machine and load at break was recorded. Figure 3.6 shows the SBS test specimen under load.



Figure 3.6. SBS test specimen and test configuration

The shear strength (τ_{max}) was calculated based on the equation;

$$\tau_{max} = \frac{0.75P_f}{bd} \quad (3.10)$$

where P_f is the failure load, b and d are the width of the specimen and thickness of the specimen, respectively.

3.3.3. Composite Sandwich Structure

3.3.3.1. Flatwise Compression Test

The flatwise compressive strength, modulus and energy absorption characteristics of the composite panels were determined according to ASTM C 365M-11a. Compression test specimens were sectioned and the tests were performed using the mechanical test machine at a crosshead speed of 0.5 mm/min. Test specimen surfaces were square with 70 mm in edge dimensions. At least five specimens were tested and force vs. displacement values were recorded using the Shimadzu™ Universal test machine. The compressive strength and modulus values were obtained by equation 3.1 and 3.3 as used for the core material.

3.3.3.2. Flatwise Tensile Test

Flatwise tensile test method (ASTM C 297M-15) was used to determine the ultimate flatwise tensile strength. Flatwise tensile test specimens were cut into square shape with 50 mm edge for each core thickness using a diamond saw. Tests (at least five specimens for each thickness) were performed by using the universal test machine with a 100 kN load cell at a crosshead speed of 0.5 mm/min. Test configuration and the specimen under flatwise tensile loading is given in Figure 3.7.

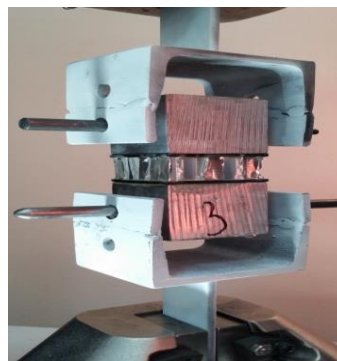


Figure 3.7. Flatwise tensile test specimen (Carbon fiber/epoxy composite/Al honeycomb sandwich) and test configuration

3.3.3.3. Edgewise Compression Test

Edgewise compression test method (ASTM C 364M-07) was used to determine the compressive properties and energy absorption characteristics of flat structural sandwich construction in a direction parallel to the sandwich face sheet. Failure modes of the composite sandwich panels were detected. Edgewise compression test specimens were cut with the dimensions given in Table 3.1 and the tests were performed using the mechanical test machine at a crosshead speed of 1.7 mm/min. At least five specimens were tested and force versus stroke values were recorded using the universal test machine. Test configuration and the specimen under edgewise compression loading is given in Figure 3.8.



Figure 3.8. Edgewise compression specimen (Carbon fiber/epoxy composite/ Al honeycomb sandwich) under loading

The ultimate edgewise compressive strength value was calculated by the equation 3.11;

$$\sigma = \frac{P_{max}}{w(2t_{fs})} \quad (3.11)$$

where, σ is ultimate edgewise compressive strength (Mpa), P_{max} is ultimate force prior to failure (N), w is width of specimen (mm) and t_{fs} is thickness of a single facesheet

(mm). Specific absorbed energy is obtained by dividing the area under the load-deformation curve by the weight.

Table 3.1. Specimen dimensions for edgewise compression test

Core thicknesses of sandwiches (mm)	6	21	46
Specimen dimensions (mm)	88x50	200x50	400(310)x50

3.3.3.4. Flexural Test

The flexural test method (ASTM C 393M-11) was used to measure the core shear stress, facing bending stress and panel bending stiffness of the composite sandwich panels. For this purpose, three point bending test specimens for each thickness were cut into 75 mm in width and 200 mm in length. Figure 3.9 shows flexural test configuration and the specimen. Tests were performed using the mechanical test machine at a crosshead speed of 5 mm/min. Spans were adjusted as 90 mm for 6 mm and 100 mm for sandwich structures those have 21 mm and 46 mm core thicknesses. At least five specimens were tested and force and displacement values were recorded using Shimadzu™ universal test machine.

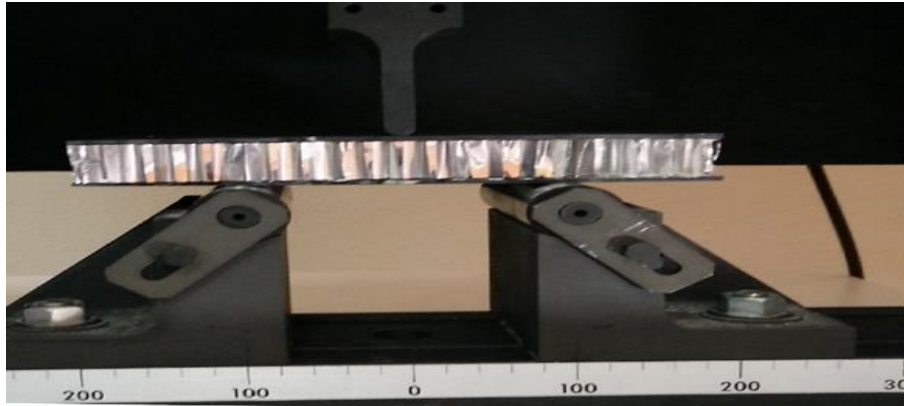


Figure 3.9. Three point bending test specimen (Carbon fiber/epoxy composite/Al honeycomb sandwich) under loading

Core shear stress (τ) values were determined by the equation below;

$$\tau = \frac{P_{max}}{(d+c)b} \quad (3.12)$$

where P_{max} is maximum force prior to failure, d is sandwich thickness, c is the core thickness and b is the sandwich width. Face sheet bending stress (σ) is obtained by the equation;

$$\sigma = \frac{P_{max}S}{2t(d+c)b} \quad (3.13)$$

where t is face sheet thickness and S is the span length. The dimensions mentioned above can be seen in Figure 3.10.

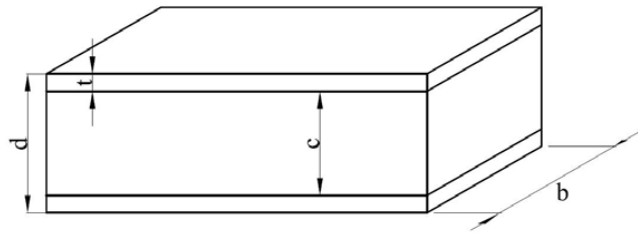


Figure 3.10. Sandwich structure dimensions

Panel bending stiffness (D) was obtained by the formula given below;

$$D = \frac{E(d^3 - c^3)b}{12} \quad (3.14)$$

$$D = \frac{E_1 t_1 E_2 t_2 (d+c)^2 b}{4(E_1 t_1 + E_2 t_2)} \quad (3.15)$$

where E is the face sheet modulus. Equation 3.14 was used for the same facings and equation 3.15 is valid for different facings. In this study, equation 3.14 is used since face sheets are identical. Sandwich beam deflection was also calculated in this test method by equation 3.16.

$$\Delta = \frac{PL^3}{48D} + \frac{PL}{4U} \quad (3.16)$$

where Δ is the total beam midspan deflection. In this formula U is the panel bending rigidity and it is calculated by the equation below;

$$U = \frac{G(d+c)^2 b}{4c} \quad (3.17)$$

where G is the core shear modulus.

3.3.3.5. Mode I Interfacial Peel Strength Test

Mode I interfacial peel strength of the composite sandwich structures were measured using ASTM D 5528-13 test method. The specimens were sectioned from large composite sandwich panels with a width of 25 mm and length of 150 mm for each core thickness. The initial peeling length, a_0 , was set to about 62.5 mm. The specimens were tested at a crosshead speed of 5 mm/min. The cross-head displacement was measured by the universal test machine. Peel strength of composite face sheet/Al core was calculated based on the load required to separate bonded materials by dividing the unit width.

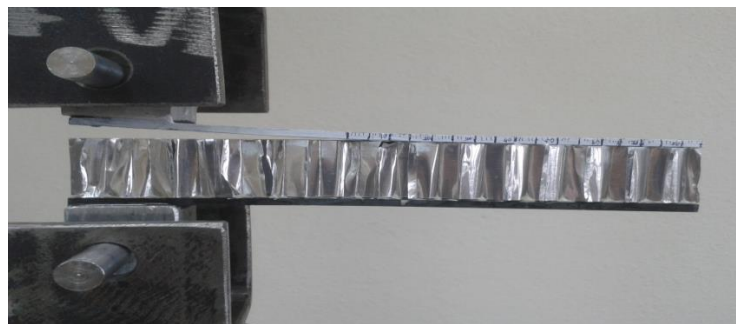


Figure 3.11. Peel test specimen under loading to determine interfacial properties

CHAPTER 4

RESULTS AND DISCUSSIONS

In this chapter, the mechanical properties of Aluminum (Al) honeycomb core materials, face sheet material and composite sandwich structure were reported in detail and the discussions were made on the structural behavior of the composite sandwich structure.

4.1. Properties of Al Honeycomb Core Materials

4.1.1. Cell Wall Thickness

The cell wall thicknesses were measured based on optical microscopy. Figure 4.1 shows optical microscope images of Al honeycomb core cross-sections. Based on the images captured, the average wall thickness was measured as $45.36 \pm 3.7 \mu\text{m}$, $43.50 \pm 1.9 \mu\text{m}$, $44.08 \pm 3.1 \mu\text{m}$ for 6, 21, 46 mm thick cores, respectively.

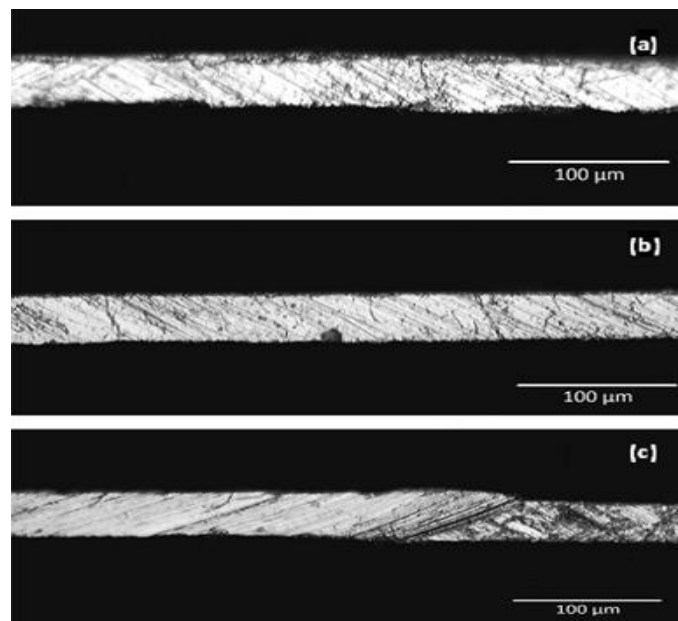


Figure 4.1. Optical microscope images of Al core material cross-sections for (a) 6 mm, (b) 21 mm and (c) 46 mm thick cores (magnification: 20X)

4.1.2. Flatwise Compression Properties

The typical force-displacement curves for Al honeycombs, with various thicknesses loaded under flatwise compression, are presented in Figures 4.2 to 4.4.

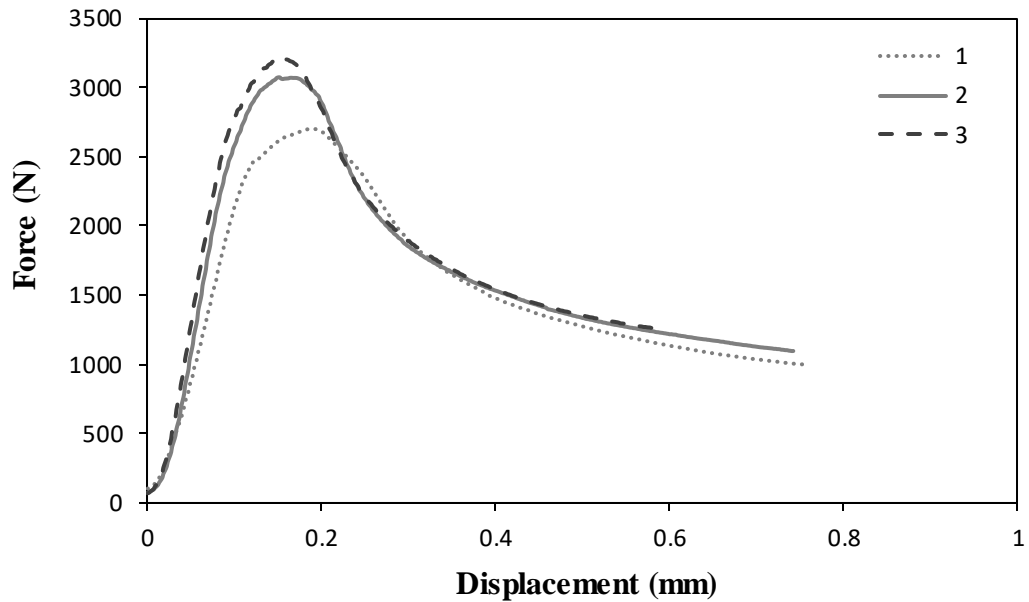


Figure 4.2. Force-displacement curves of Al based honeycomb core materials under flatwise compression (core thickness is 6 mm)

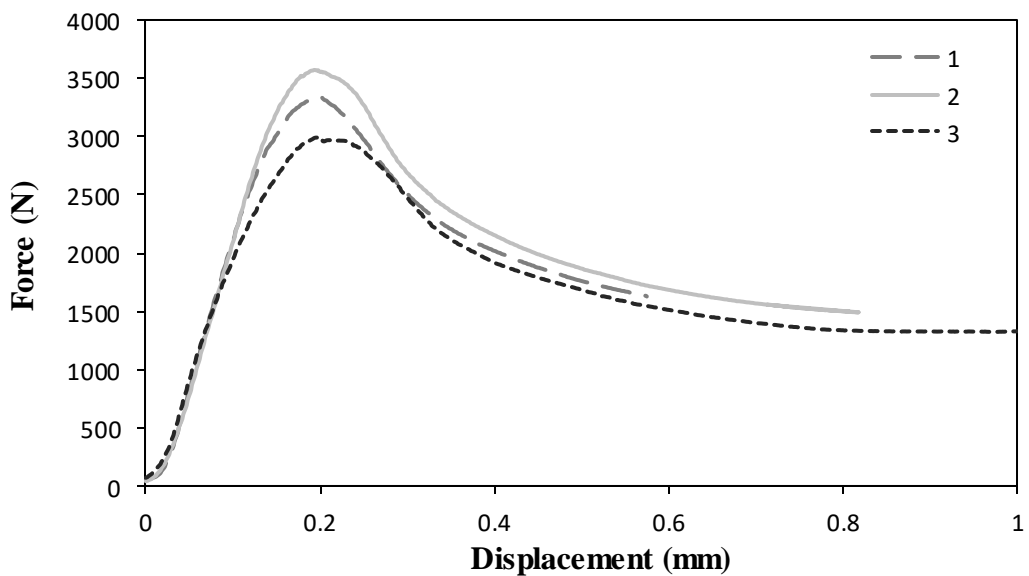


Figure 4.3. Force-displacement curves of Al based honeycomb core materials under flatwise compression (core thickness is 21 mm)

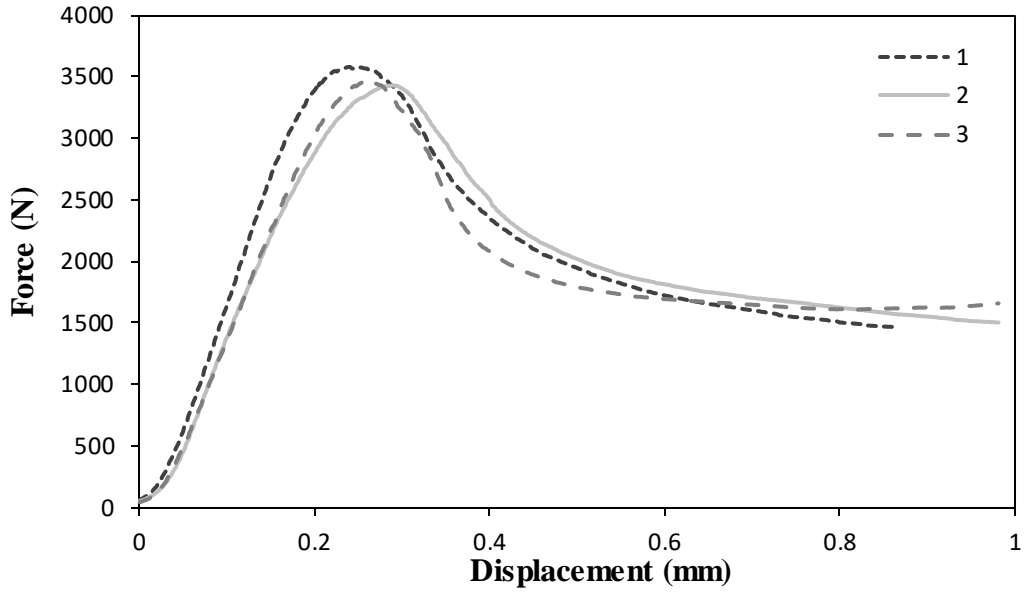


Figure 4.4. Force-displacement curves of Al based honeycomb core materials under flatwise compression (core thickness is 46 mm)

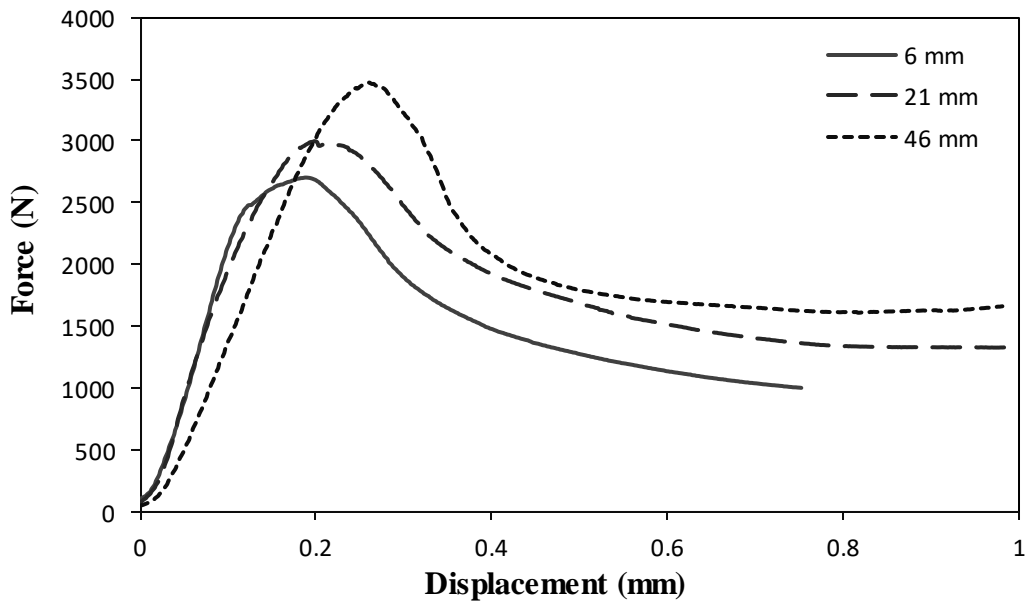


Figure 4.5. Comparison of typical flatwise compressive behavior of Al based honeycomb core materials for various core thicknesses

Figure 4.5 shows the comparison of force-displacement curves of Al honeycomb core materials for three different core thicknesses under flatwise compression. All specimens showed similar trend at the initial stage of the compression loading. Up to some displacement level, core materials exhibit elastic deformation behavior. After certain values, the core cell walls start to buckle and then sudden collapse occurs. As the core

thickness increases, the maximum force levels were observed to increase slightly. Deformation modes of the Al core materials are shown in Figure 4.6. It was observed that buckling and crushing on the core cell walls occurred due to the main mechanisms within the cores during the flatwise compression loading. It was also observed that the failure modes of the core deformation alter due to the change of core thicknesses. The average flatwise compressive strength and modulus are also summarized in Table 4.1 as a function of the core thickness. It was found that the compressive strength and modulus values of Al honeycomb increase as the core thickness increases.

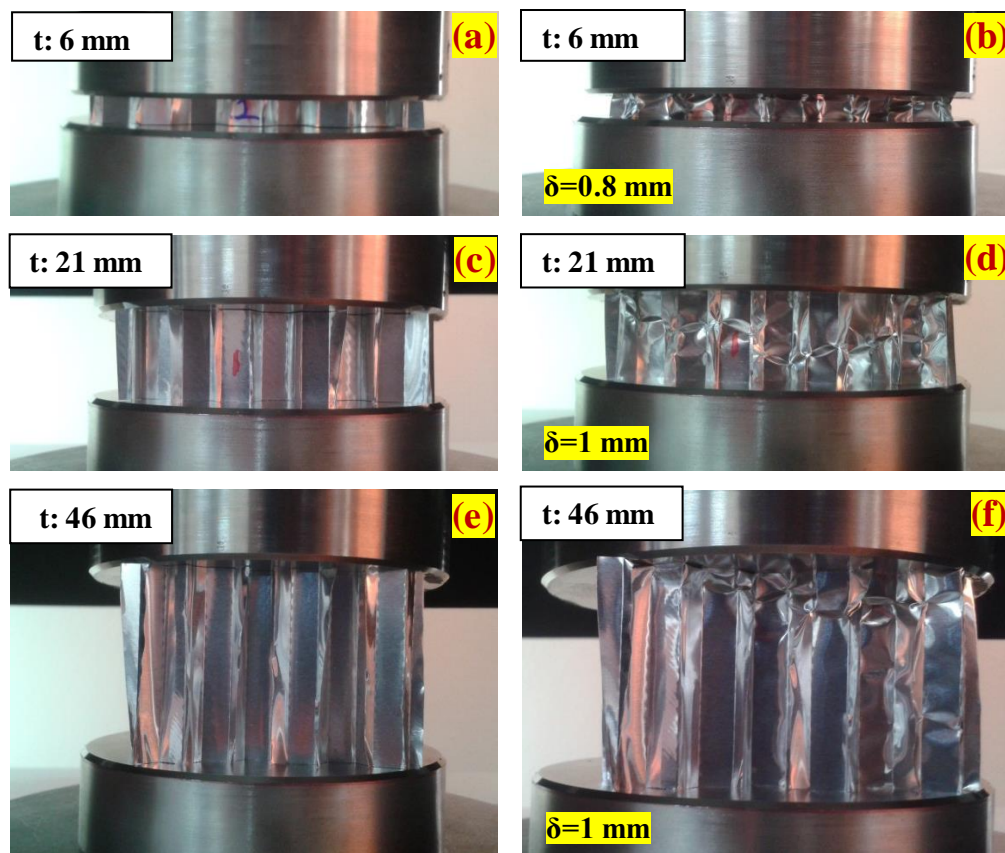


Figure 4.6. Images of flatwise compression test specimens; before (a-c-e) and after (b-d-f) loading (δ = displacement in mm) (t is core thickness in mm).

Table 4.1. Summary of flatwise compression test results of Al honeycomb core.

Core thickness (mm)	Elastic Modulus (MPa)	Strength (MPa)
6	38 ± 7.4	0.62 ± 0.02
21	100 ± 20.6	0.67 ± 0.05
46	148.7 ± 16	0.70 ± 0.01

4.2. Properties of Face Sheet Material

4.2.1. Fiber Volume Fraction

The fiber volume fraction values of the carbon fiber/epoxy composite face sheets were measured by using Archimedes' Principle as given in Table 4.2, the average fiber volume fraction (V_f) was calculated as 54 ± 1.3 for the composite face sheets manufactured.

Table 4.2. Fiber volume fraction of face sheets manufactured

Sample No	W_{air} (g)	W_{water} (g)	Composite Density (g/cm^3)	Fiber Volume Fraction (V_f)
1	1.28	0.39	1.44	0.55
2	1.40	0.42	1.43	0.54
3	1.39	0.42	1.44	0.55
4	1.33	0.40	1.43	0.54
5	1.46	0.43	1.42	0.52
Average	1.37	0.41	1.43	0.54
Std. Dev. (+/-)	0.07	0.01	0.008	0.013

4.2.2. Tensile Test Results

Figure 4.7 shows the tensile stress-strain curves of carbon fiber/epoxy composite face sheets. Stress-strain response of the composite face sheet is almost linear up to the maximum stress values reached, and then the complete failure of the specimens occur followed by a sudden load drop. In the initial stage, the composite exhibits elastic deformation behavior and fracture start near to maximum stress level. As seen in Table 4.3., the average ultimate axial strength, modulus and failure strain values of the face sheets were found to be 671.7 ± 15.5 MPa, 61.4 ± 4 GPa and 1.06 ± 0.07 , respectively.

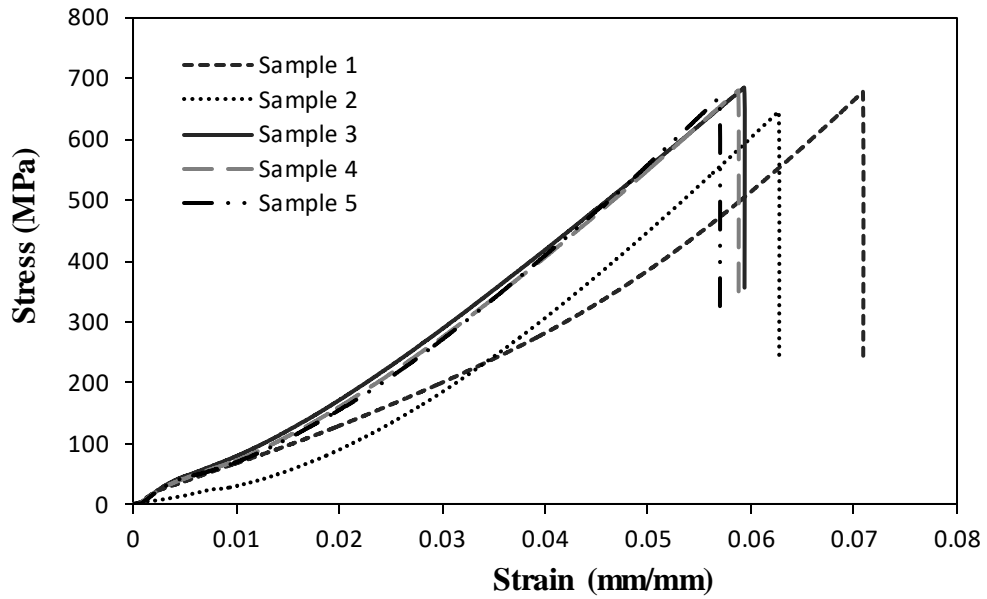


Figure 4.7. Stress-strain curves of carbon/epoxy composite face sheets under tensile loading

Table 4.3. Summary of tensile properties of carbon/epoxy composite face sheets

Sample No	Ult. Axial Tensile Strength (σ_{11}) (MPa)	Axial Tensile Modulus (E_{11}) (GPa)	Axial Failure Strain (ϵ_{11}) (%)
1	678.1	55.4	1.18
2	646.0	66.4	0.98
3	685.2	59.9	1.09
4	680.4	62.6	1.06
5	668.9	62.5	1.02
Average	671.7	61.4	1.06
Std.Dev. (+/-)	15.5	4.0	0.07



Figure 4.8. Tensile test specimen and set-up (left) and the failed test specimen (right)

4.2.3. Compression Test Results

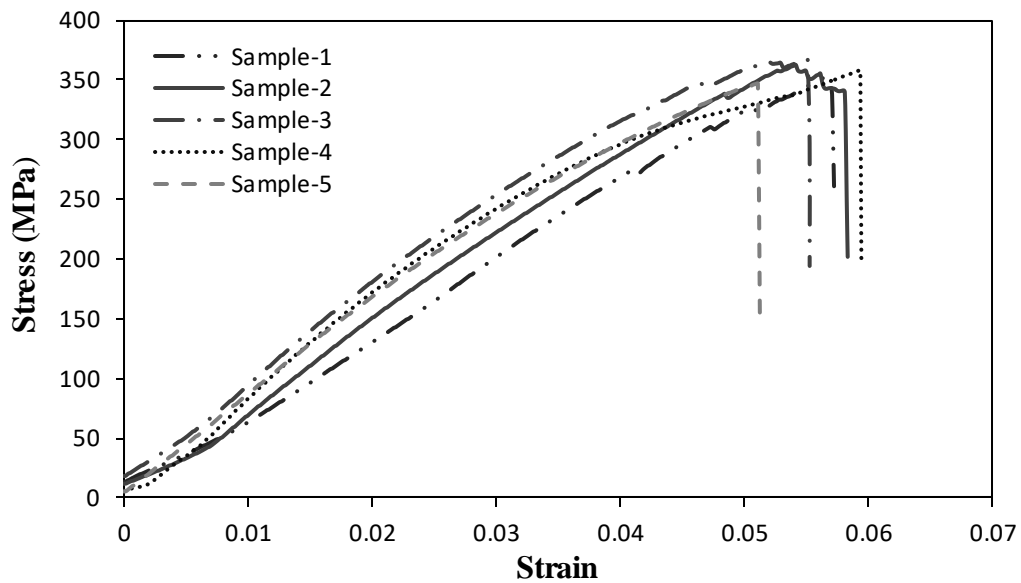


Figure 4.9. Stress-strain curves of composite face sheets under compression

The compressive stress-strain curves of the composite face sheets are shown in Figure 4.9. As seen in the figure, composites exhibit almost linear behavior due to elastic deformation up to the maximum stress levels. At the maximum level, failure of the composites occurs. Figure 4.10 shows the compression test set-up and failure mode of the specimens. It was observed that the specimens failed with buckling and shear deformations. It is note-worthy that the observed failure modes are the acceptable ones for compression test. Test results are given in Table 4.4 and the average compressive strength, modulus and failure strain values were found to be 367.81 ± 24.85 MPa, 7.89 ± 0.67 GPa and 0.46 ± 0.06 , respectively.

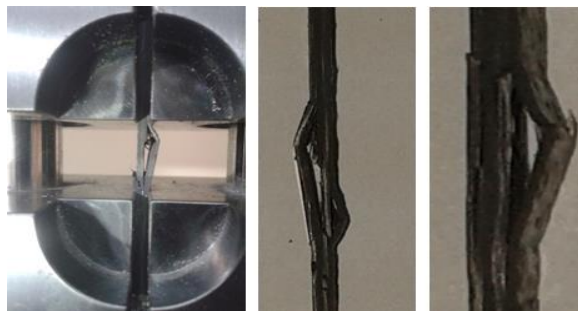


Figure 4.10. The images of the compression test set-up (left) and the test specimen after compressive loading (middle, right)

Table 4.4. Summary of compression test results of carbon/epoxy composite

Sample No	Ult. Axial Compressive Strength (σ_{11}) (MPa)	Axial Compressive Modulus (E_{11}) (GPa)	Axial Break Strain (ϵ_{11}) (%)
1	352.04	6.87	0.44
2	362.59	7.97	0.44
3	367.66	8.10	0.43
4	409.78	8.68	0.57
5	346.98	8.10	0.40
Average	367.81	7.89	0.46
Std. Dv. (+/-)	24.85	0.66	0.06

4.2.4. Flexural Test Results

Flexural stress-strain curves of the specimens are given in Figure 4.11. It is observed that increase in stress levels is linear in the elastic region and the maximum stress occurs at the mid span as expected. After the maximum stress was reached, specimens are failed as illustrated in Figure 4.12 and stress value drops suddenly. The average flexural strength and modulus values were found to be 640.52 ± 35.95 MPa and 42.03 ± 5.43 GPa, respectively, as listed in Table 4.5. The average bending strain value was found to be 1.55 ± 0.14 .

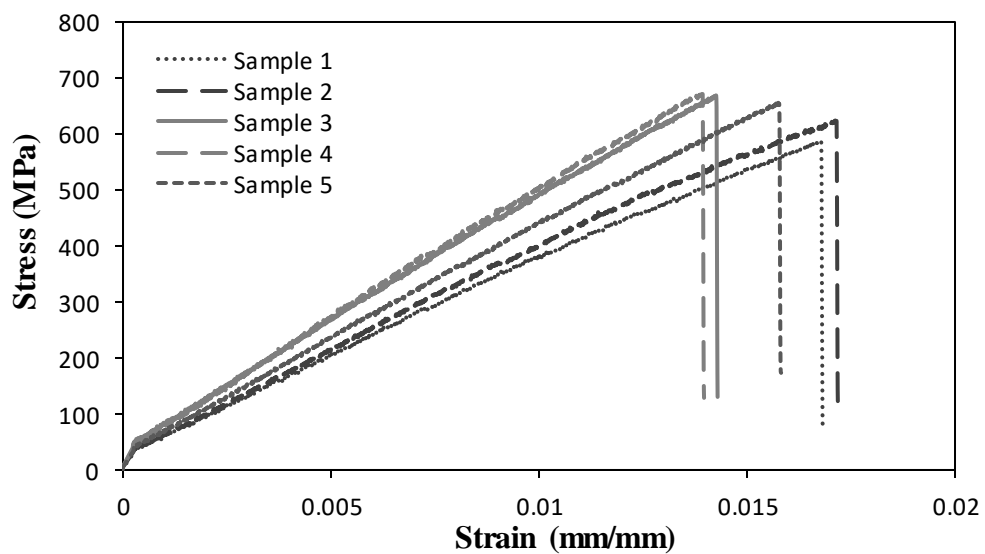


Figure 4.11. Flexural stress-strain curves of composite face sheet under three-point bending

Table 4.5. Summary of flexural test results for carbon/epoxy composite

Sample No	Flexural Strength (MPa)	Flexural Modulus (GPa)	Flexural Strain (%)
1	585.6	35.79	1.68
2	623.3	37.81	1.71
3	667.8	46.49	1.43
4	670.3	48.45	1.40
5	655.6	41.63	1.57
Average	640.52	42.03	1.55
Std. Dv. (+/-)	35.95	5.43	0.14

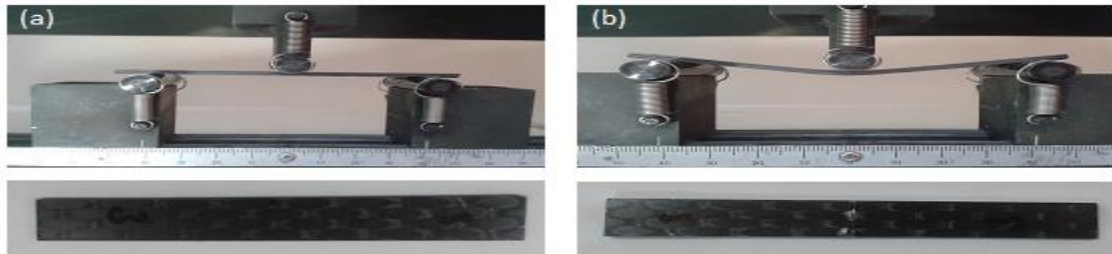


Figure 4.12. The images of flexural test specimen (a) before and (b) after bending test

4.2.5. Interlaminar Shear Strength (ILSS) of the composite

The average inter laminar shear strength value of the face sheets was found to be 39.3 ± 1.8 MPa (Table 4.6). The typical failure mode was observed to be the shear failure of the composite at interlaminar region.

Table 4.6. Summary of ILSS test results of carbon/epoxy composite

Sample No	Max. Force (N)	ILSS (MPa)
1	981.2	40.6
2	931.2	38.3
3	868.2	36.6
4	1009.3	39.8
5	926.5	41.2
Average	943.3	39.3
Std. Dv. (+/-)	54.4	1.8

4.3. Mechanical Behavior of Composite Sandwich Structures

4.3.1. Flatwise Compressive Behavior of Sandwich Structures

Load-displacement curves of carbon/epoxy faced/Al honeycomb core based composite sandwich structures under flatwise compression are shown in Figures 4.13 to 4.15. As seen in the figures, the forces initially increase linearly. A relatively large drop of the force was observed, followed by a plateau region in which the stress was almost constant as the deformation is progressed. Above the maximum force level, the cell walls collapse suddenly due to the bending and local buckling of the cell walls. Force-displacement curves of composite sandwich structures for various core thicknesses are given in Figure 4.16. As seen in the figure, the maximum load level decreases gradually with increasing the core thickness of composite sandwich structures. Bending and local buckling of the cell walls occurs at lower load levels as the thickness of the core increases. This results with a decrease in compressive strength of the sandwich structures that is manufactured with relatively thicker core materials. After some displacement level, the sandwiches continue to crush in cells walls and the buckling continues simultaneously. A relatively higher energy absorption values were calculated for the sandwiches containing thicker cores. The average specific absorbed energies ($E_{s,a}$), were calculated as 0.06 ± 0.002 , 0.055 ± 0.001 and 0.057 ± 0.003 kJ/kg for sandwiches containing 6, 21, 46 mm thick cores, respectively (The given values were calculated for compression of the sandwiches up to 1.5 mm).

Failure mechanisms of the composite sandwich structures during compressive loading were also examined as illustrated in Figure 4.17. It was seen that cell wall crushing and core buckling are the main mechanisms occurred within the sandwiches due to flatwise compression. It was also seen that the failure modes of the Al core deformation alters due to the change of core thicknesses.

After the maximum load level, a large drop of the force values was observed followed by the plateau region where the stress was almost constant during progress of deformation. This increase in force level at this region is due to the densification of the folded cell walls (Tuwair, 2015). In Figure 4.18.b, an example graph of specific absorbed energy (absorbed energy/weight of the composite, $E_{s,a}$) is also illustrated. The deformation of the structure under compressive load is illustrated by the images given in

Figure 4.18.a. After the maximum load level, bending and crushing of the cell walls continue with increasing deformation as shown in the figures from left to the right.

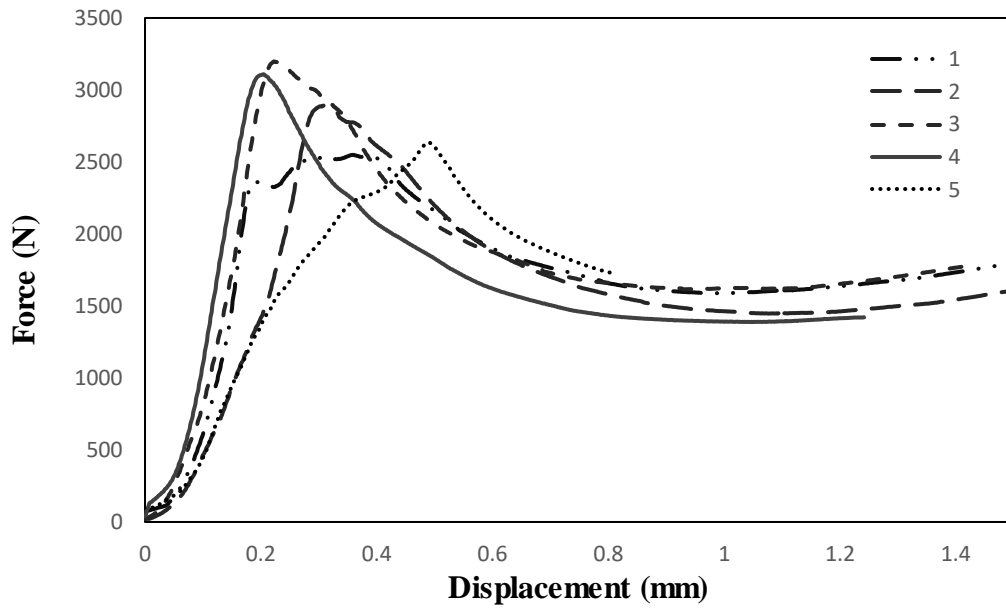


Figure 4.13. Force-displacement curves of composite sandwich structure under flatwise compression (Al honeycomb core thickness is 6 mm)

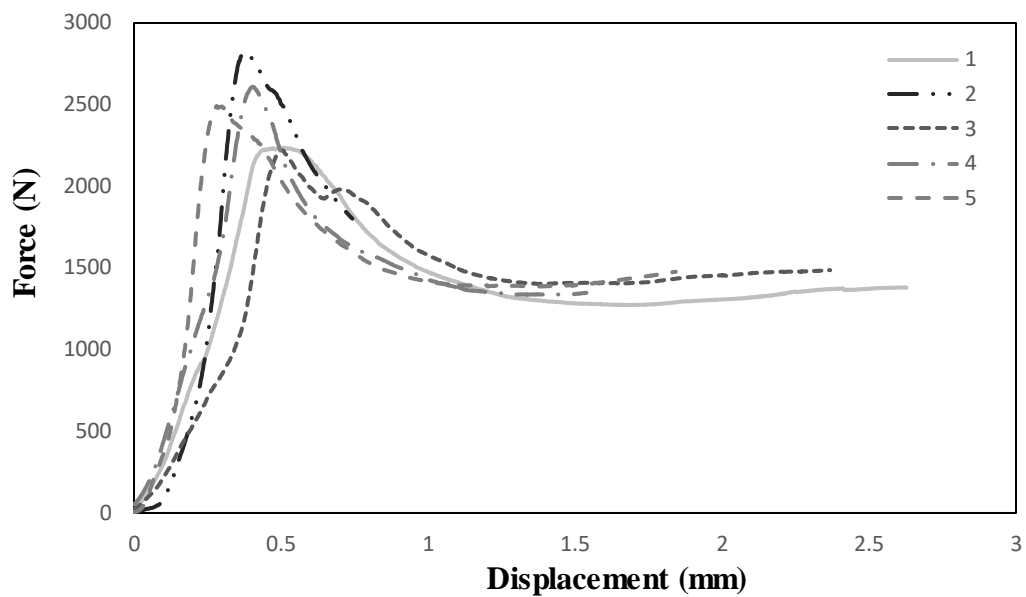


Figure 4.14. Force-displacement curves of composite sandwich structure under flatwise compression (Al honeycomb core thickness is 21 mm)

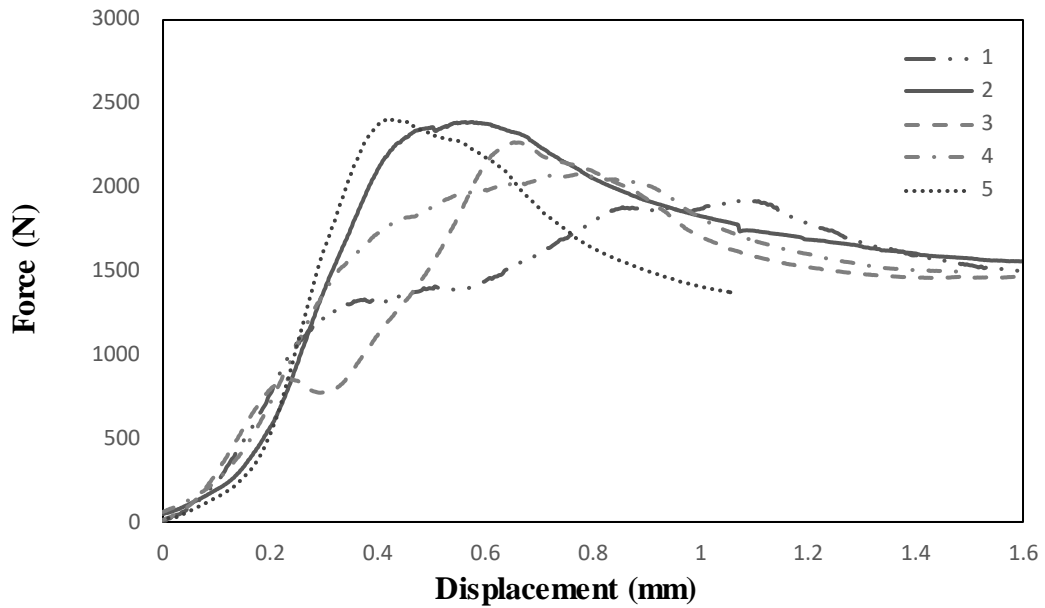


Figure 4.15. Force-displacement curves of composite sandwich structure under flatwise compression (Al honeycomb core thickness is 46 mm)

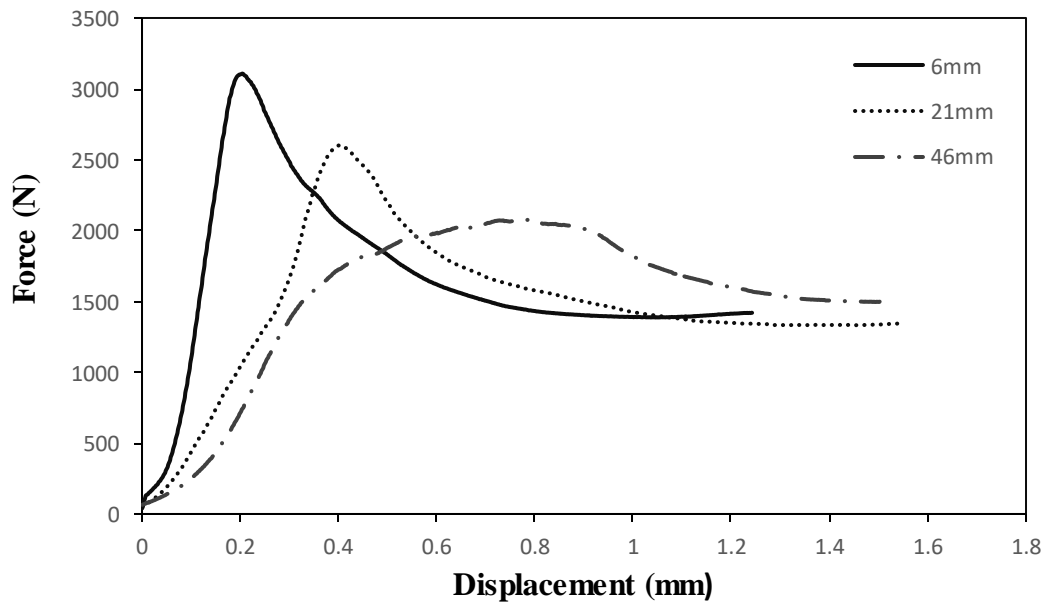


Figure 4.16. Typical force-displacement curves of composite sandwich structures for various core thicknesses obtained from the flatwise compression tests

The average flatwise compression strength and modulus values of composite sandwich structures for various core thicknesses are presented in Table 4.7. Although the strength values decrease, the compressive modulus values were found to be increased due to the increase in core thickness.

Table 4.7. Summary of flatwise compression test results for carbon-epoxy/Al honeycomb composite sandwich structures with various core thicknesses

Core thickness (mm)	Elastic Modulus (MPa)	Compressive Strength (MPa)
6	13.52 ± 3.00	0.56 ± 0.094
21	18.20 ± 5.41	0.44 ± 0.080
46	45.00 ± 12.8	0.41 ± 0.045

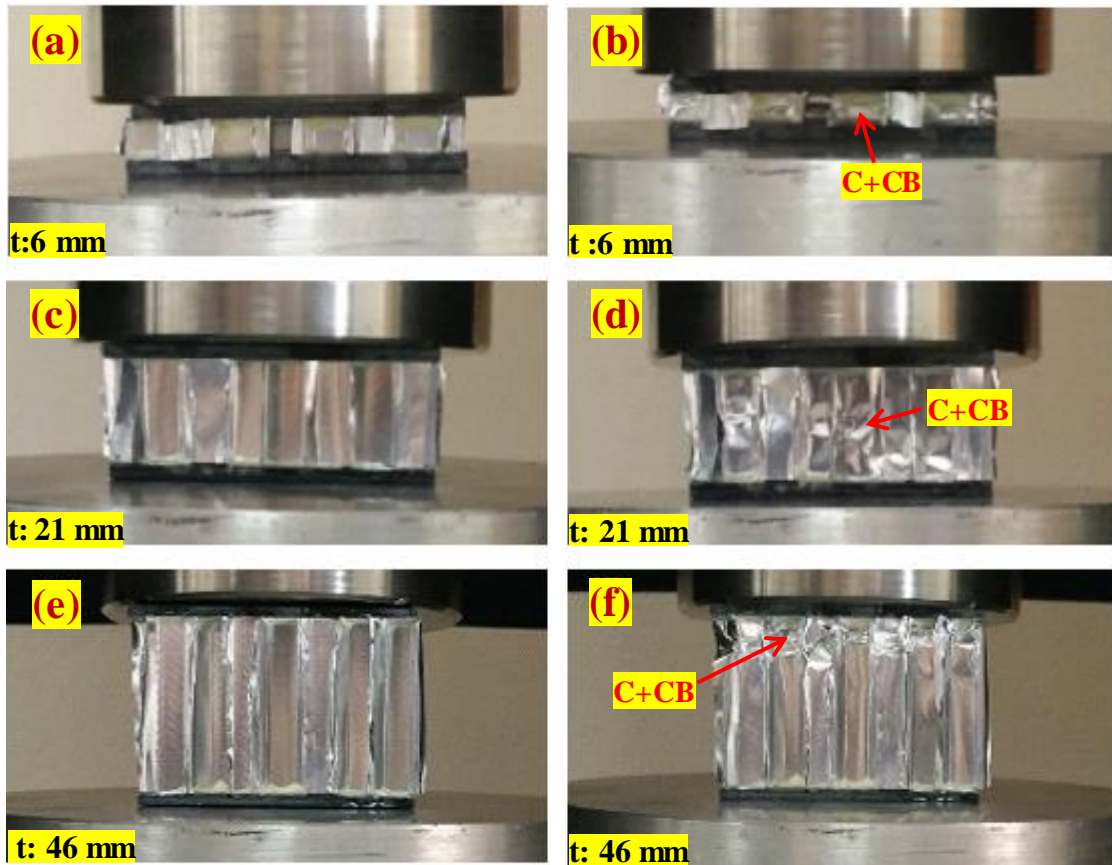


Figure 4.17. The images of flatwise compression test samples of the composite sandwich structures; before (a-c-e) and (b-d-f) after the tests (C: crushing, CB: core buckling) (t is core thickness in mm)

Collapse sequence images and representative force-displacement curve and the corresponding specific absorbed energy ($E_{s,a}$) graph of the composite sandwich structure under flatwise compression are presented in Figure 4.18.

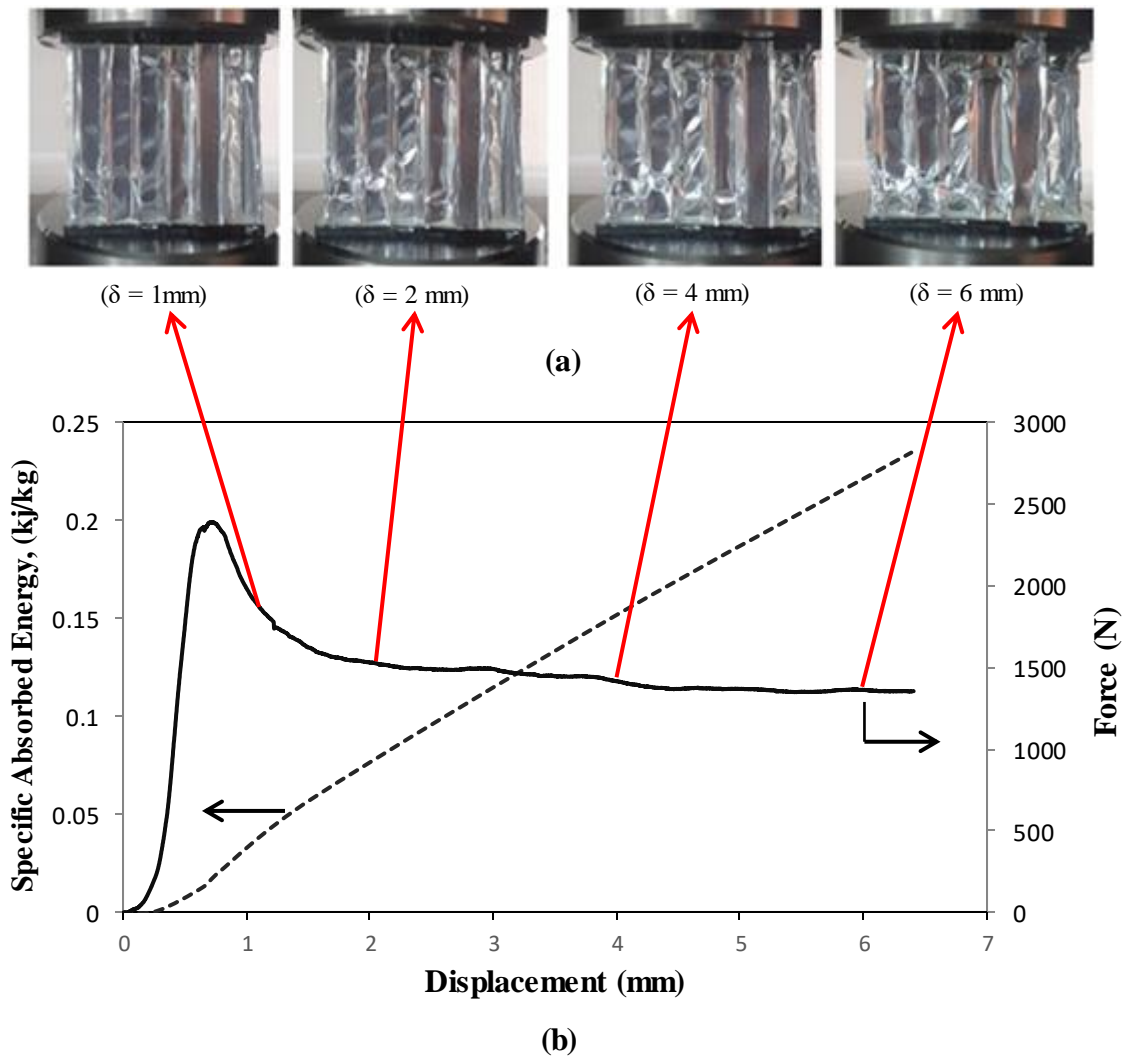


Figure 4.18. (a) Collapse sequence images and (b) representative force-displacement curve and the specific absorbed energy ($E_{s,a}$), graph of the composite sandwich structures under flatwise compression (core thickness is 46 mm)

4.3.2. Flatwise Tensile Behavior of Sandwich Structure

For flatwise tensile loading, the force-displacement curves of carbon-epoxy/ Al honeycomb composite sandwich structures for various core thicknesses were obtained as shown in Figures 4.19 to 4.21. Response of the material is almost linear up to the failure point and it exhibits elastic behavior in this range. Additionally, some scattering was observed in force- displacement curves of the sandwich specimens that may be related with non-uniform bonding not consistent because of the manufacturing imperfection adhesive bonding of the specimens.

As failure mode, adhesive failure occurred at the composite face sheet/Al core interface due to Mode I flatwise tensile loading of the sandwiches, as seen in Figure 4.22. As described before, PU based adhesive glue was used to bond face sheets and core materials together. Due to relatively lower strength of the bonding region, interfacial failure occurred. The average ultimate tensile strength and maximum force values for sandwich structures with different core thicknesses are given in Table 4.8.

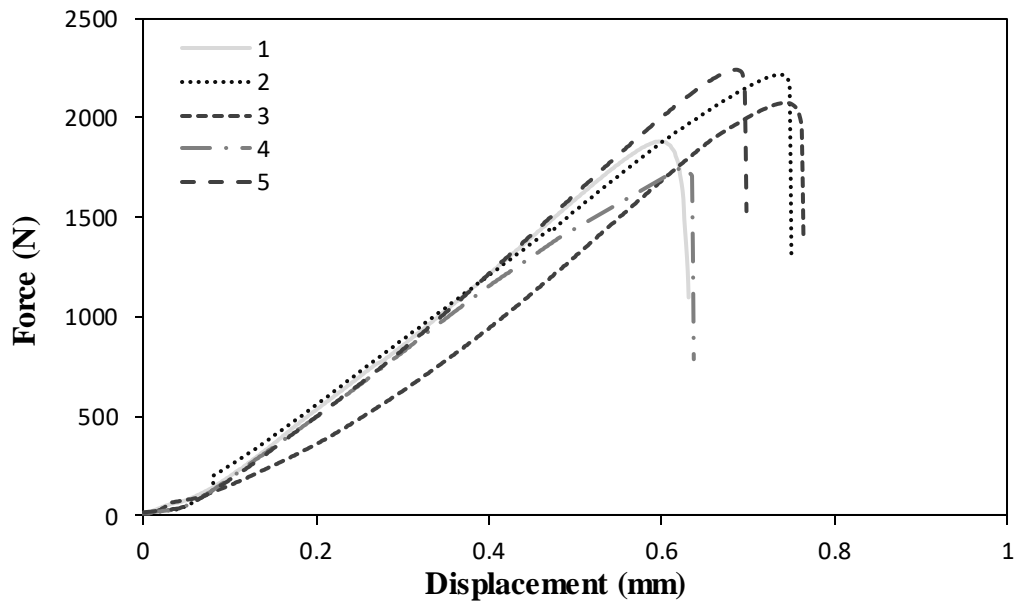


Figure 4.19. Force-displacement curves of the composite sandwich structures under flatwise tension (core thickness is 6 mm)

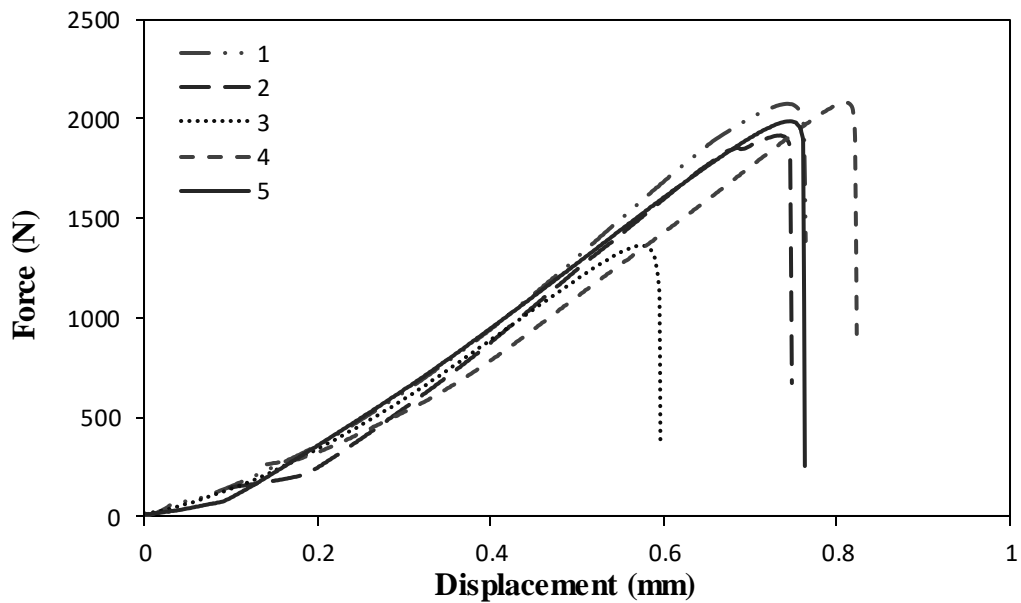


Figure 4.20. Force-displacement curves of the composite sandwich structures under flatwise tension (core thickness is 21 mm)

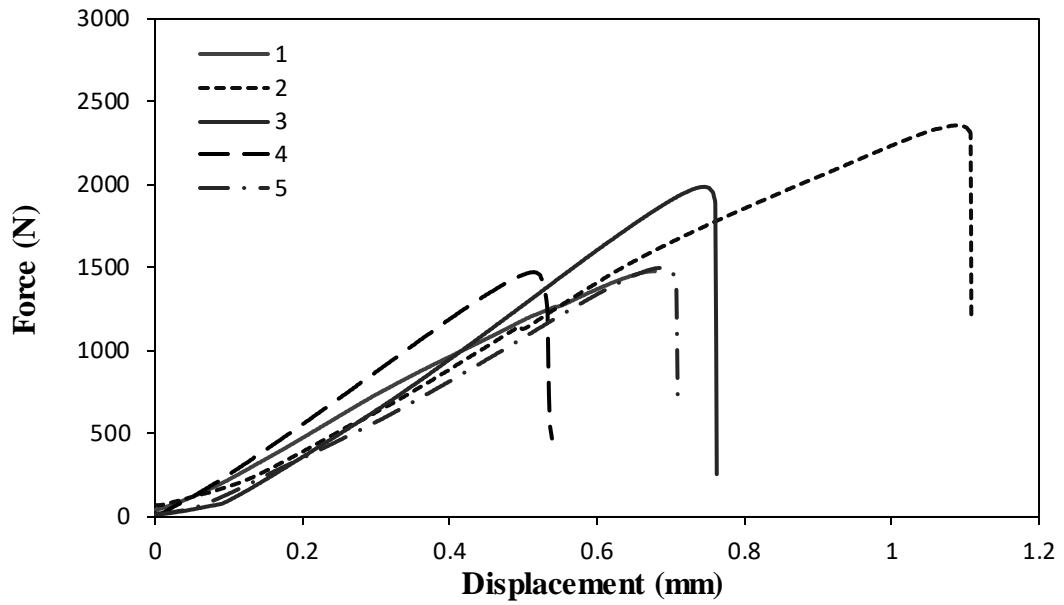


Figure 4.21. Force-displacement curves of the composite sandwich structures under flatwise tension (core thickness is 46 mm)

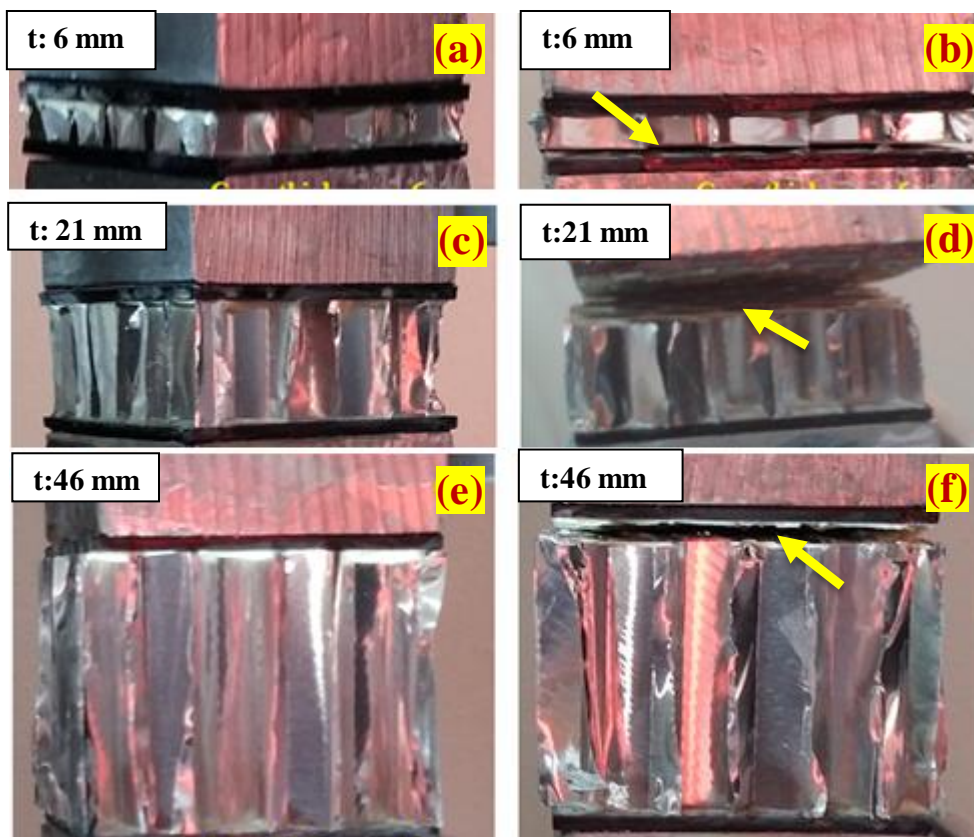


Figure 4.22. Images of flatwise tensile test specimen of the composite sandwich structures; before (a-c-e) and (b-d-f) after the tests (Interfacial failure region within the specimens are visible) (t: core thickness in mm)

Table 4.8. Summary of flatwise tensile test results for composite sandwich structures with various core thicknesses

Core thickness (mm)	Max. Force (N)	Ultimate Strength (Mode I opening) (MPa)
6	1943 ± 387	0.76 ± 0.15
21	1728 ± 370	0.67 ± 0.14
46	1510 ± 574	0.59 ± 0.22

4.3.3. Edgewise Compression Test of the Sandwich Structures

Force-displacement curves of the sandwich specimens under edgewise compression are given in Figures 4.23 to 4.25. It was seen that all of the specimens exhibit similar behavior (pseudo-linear) up to some deformation level and near to maximum force level at which the buckling of the sandwich starts. From Figures 4.23 and 4.27.b, it can be seen that the composite sandwich structure with 6 mm core bears the ultimate load followed by the complete failure. Failure mode was a combination of general buckling and interfacial de-bonding due to the shear at the interface between the core and the face sheet laminate. This collapse mode is known as ‘sandwich panel column buckling’ as described similarly by Mamalis et al. (2005).

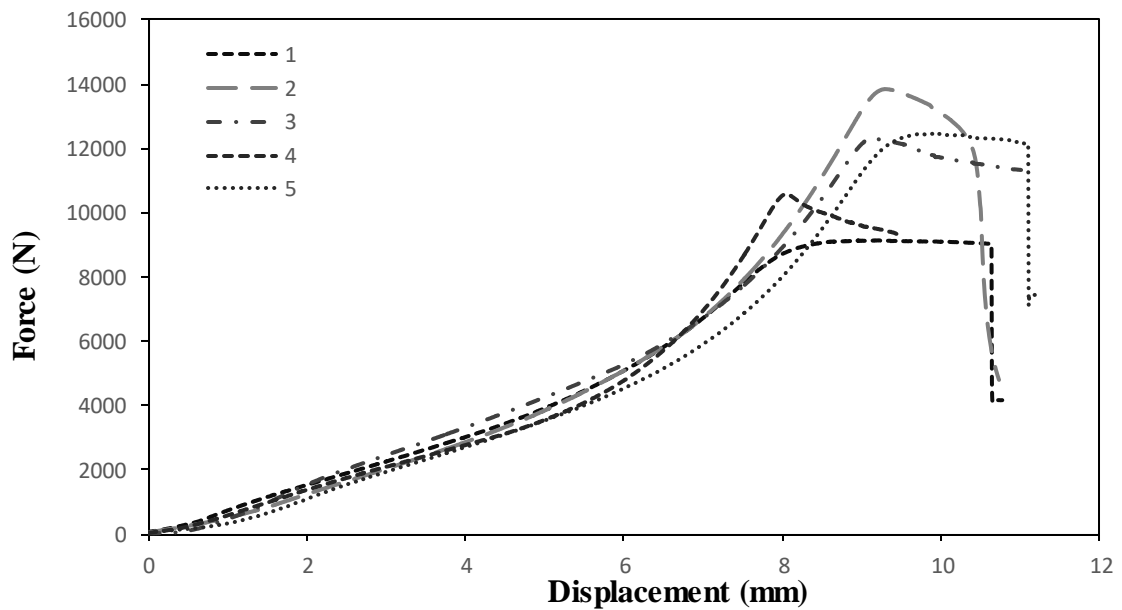


Figure 4.23. Force-displacement curves of the composite sandwich structures under edgewise compression (core thickness is 6 mm)

From Figures 4.24 and 4.27.b, it was seen that the composite sandwich structure with 21 mm core continued to carry the applied load until the ultimate load was reached. Al core crushed because of the shear at the interface between the core and the face sheet laminate. Afterwards, buckling and debonding at the interfacial region with a sudden drop of force was observed.

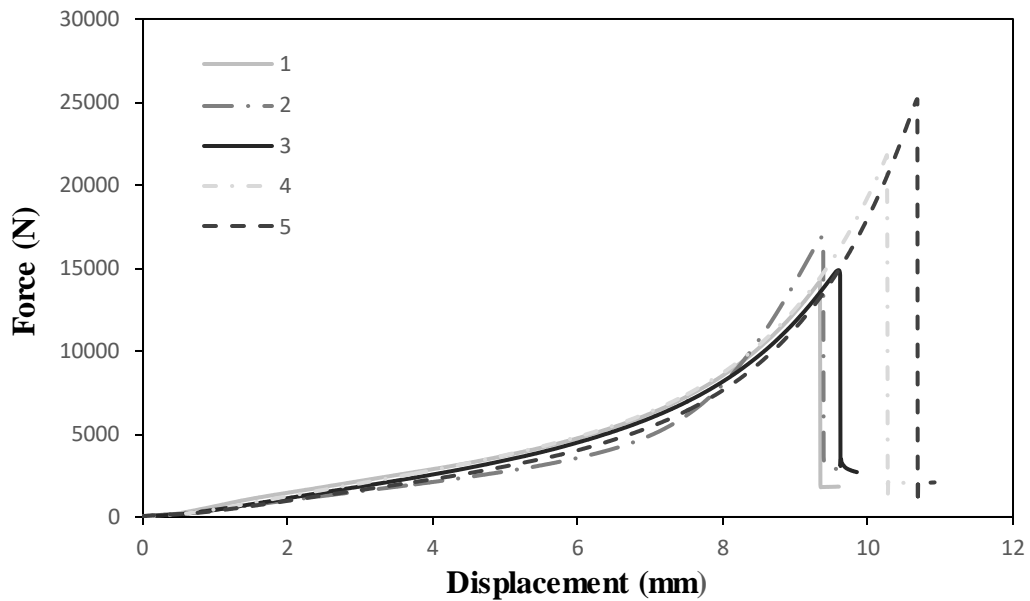


Figure 4.24. Force-displacement curves of the composite sandwich structures under edgewise compression (core thickness is 21 mm)

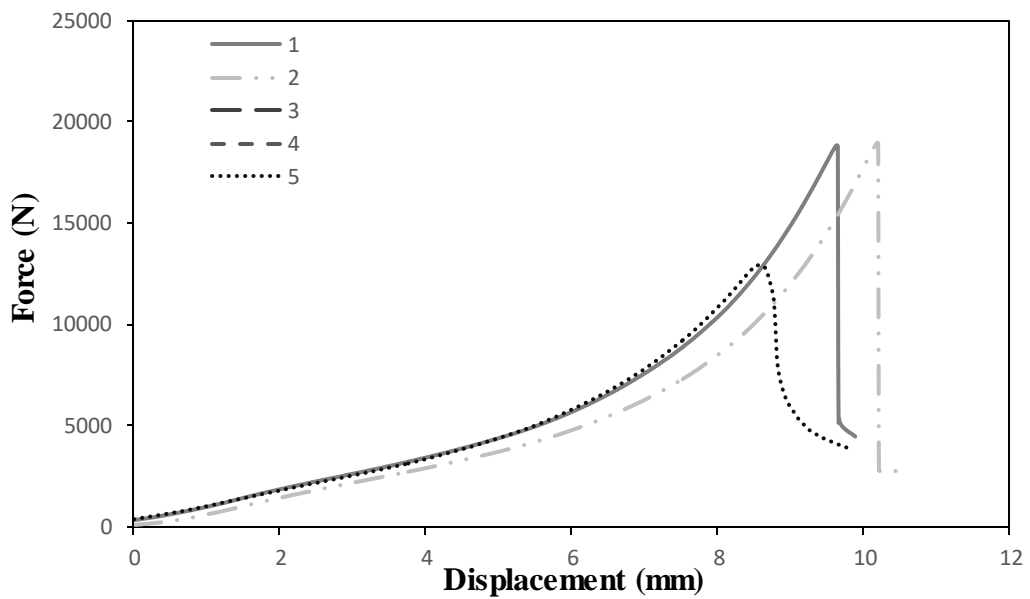


Figure 4.25. Force-displacement curves of the composite sandwich structures under edgewise compression (core thickness is 46 mm)

From Figures 4.25 and 4.27.f, it is seen that the composite sandwich structure with 46 mm core bears until ultimate loading and Al core crushes because of shear at the interface between the core and the face sheet laminate. Then, failure occurs due to general buckling and a large drop at load level. As illustrated in Figure 4.27.f, the core was subjected to shear stress during the test, the failure occurred at the end of the specimens, and then propagated through the sandwich structure. It was also observed that the load bearing capacity of the structure dramatically decreased after initial failure. A higher force level is needed for propagation of the damage and this results with a high energy absorption to structure (Lindström 2007). Comparison of typical edgewise compressive behavior of the composite sandwich structures for different core thicknesses is shown in Figure 4.26.

For composite sandwich structures with various core thicknesses, the ultimate edgewise compressive strength and specific absorbed energy obtained from force-displacement curves were calculated and summarized in Table 4.9. It was found that the energy absorption capacity of the composite sandwich structures increases with the increase of the core thickness.

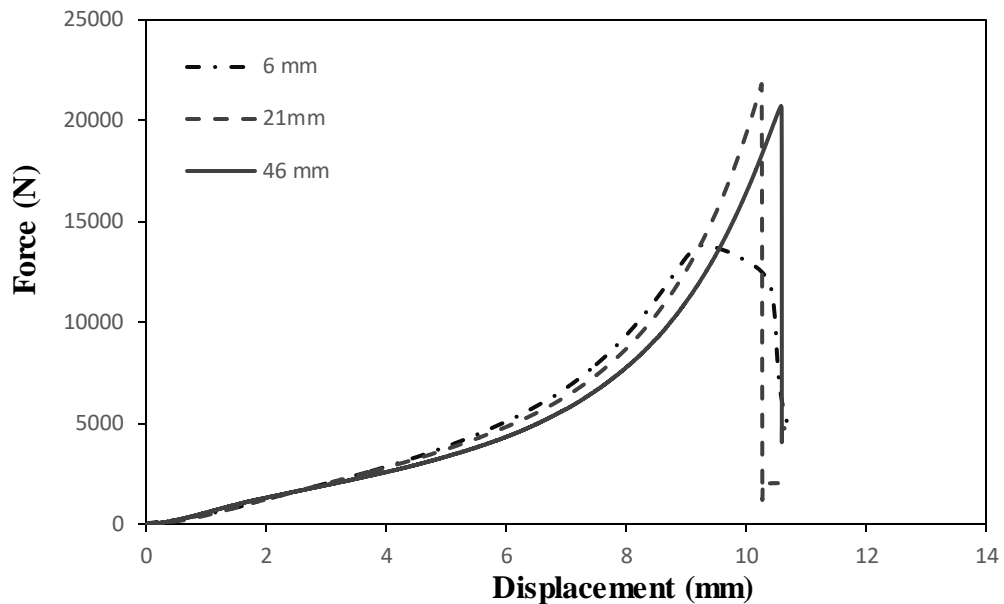


Figure 4.26. Comparison of typical edgewise compressive behavior of the composite sandwich structures for various core thicknesses

Table 4.9. The ultimate edgewise compressive strength and specific absorbed energy, $E_{s,a}$ of the composite sandwich structures with different core thickness

Core thickness of the sandwich composite (mm)	Ultimate Compressive Strength (MPa)	Specific Absorbed Energy, $E_{s,a}$ (kJ/kg)
6	37.8 ± 3.2	0.71 ± 0.1
21	67.8 ± 15.6	0.82 ± 0.1
46	72.2 ± 15.3	1.38 ± 0.4

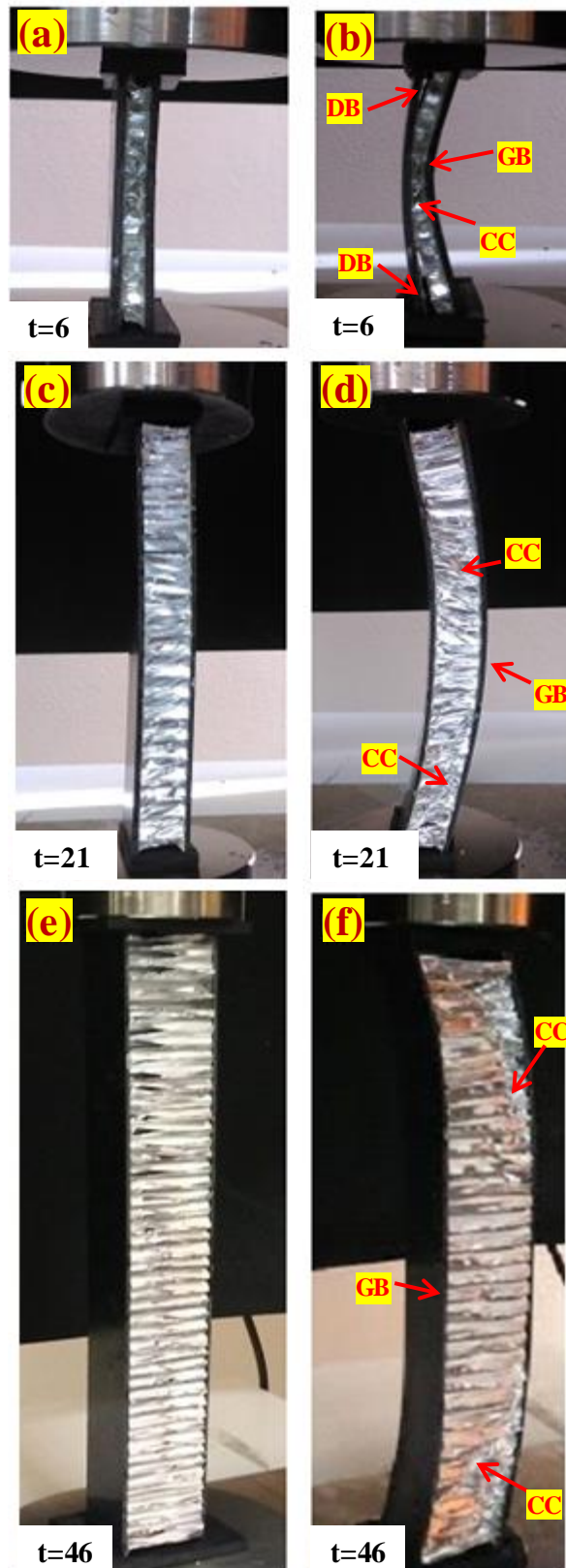


Figure 4.27. Images of edgewise compression test specimens; before (a-c-e) and after (b-d-f) the tests (CC: core crushing, GB: global buckling, DB: debonding) (t is the thickness of the core in mm)

4.3.4. Flexural Test Result of the Sandwich Structure

Figures 4.28 to 4.30 show flexural bending force-displacement curves of the composite sandwich structures for different core thickness. Comparison of typical flexural behavior of composite sandwich structures for various core thicknesses are also presented in Figure 4.31. It was observed that each sandwich structure has similar force-displacement curves and exhibited similar flexural behavior, however, the sandwich structure with 6 mm Al core exhibits relatively higher bending loads than those for other samples. All specimens failed because of the inward local bending of the compression facing beneath the loading point, as shown in Figure 4.32. The failure progressed by crushing in the top facing and the core. The core's compressive strength and stiffness were inadequate to resist high local stresses; therefore, the local bending occurred (Tuwair 2015). Flexural cracks in the core were observed at the top of the sandwich beam, however these cracks did not cause sudden failure. Final failure of the sandwich beam is due to compressive failure of the fiber composite skin followed by the debonding between the compressive skin and the core. This behavior is similar to the observation made by Manola et al. (2012). In their study, interface bond collapse occurred on sandwich structure once compressive failure was observed at the skin. There was also no visible failure of the bottom skin under tension (Manola et al. 2012). Summary of the flexural test results of the composite sandwich structure is given in Table 4.10. The maximum core shear stresses and beam deflection decreased as the core thickness increases. On the other hand, it can be noted that the bending stiffness and panel shear rigidity increases while face sheet bending stress decreased with increasing core thickness.

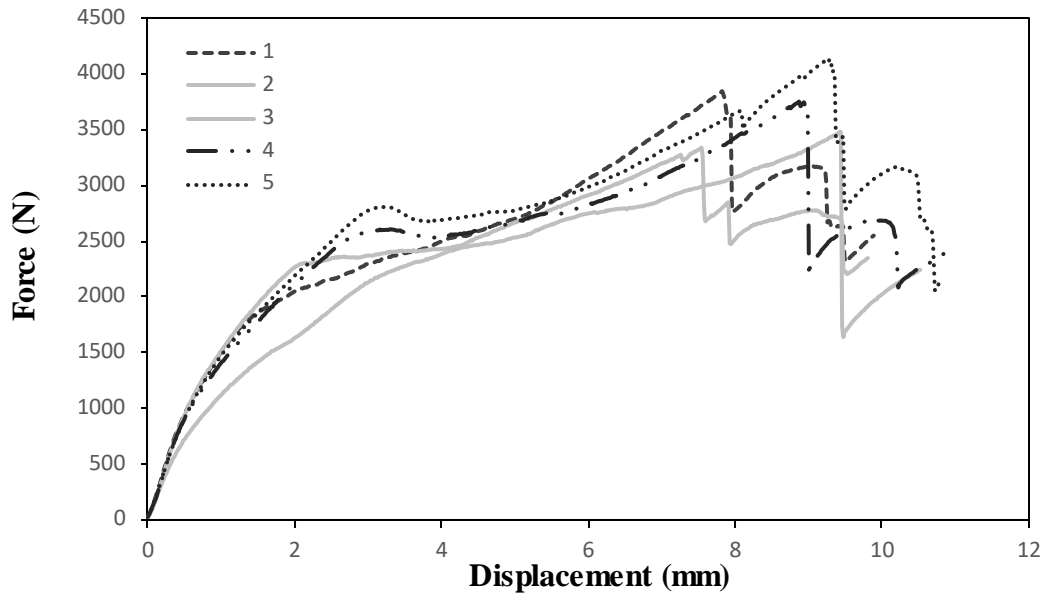


Figure 4.28. Force-displacement curves of composite sandwich structures under flexural loading (core thickness is 6 mm)

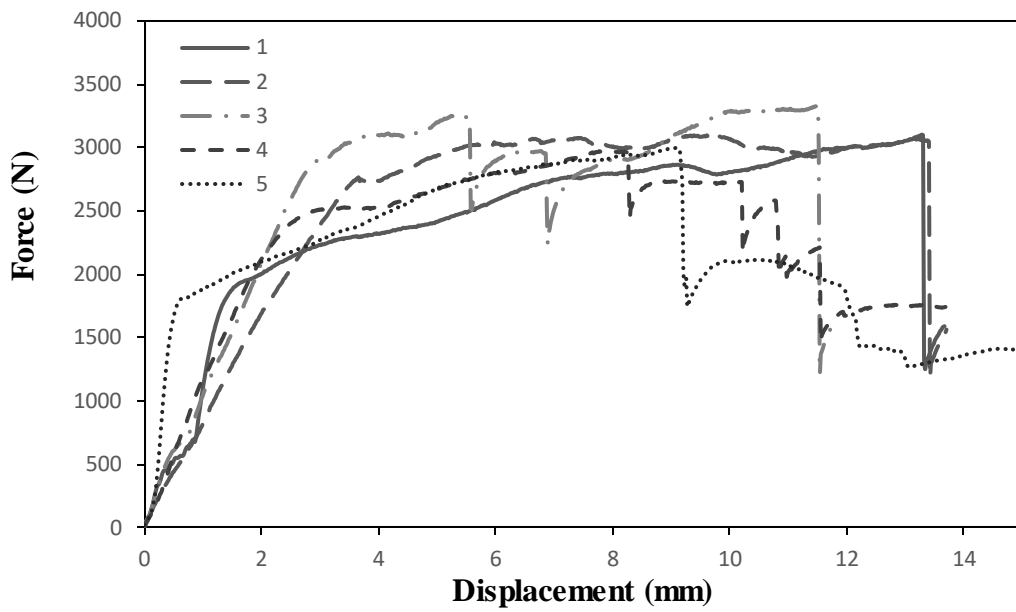


Figure 4.29. Force-displacement curves of composite sandwich structures under flexural loading (core thickness is 21 mm)

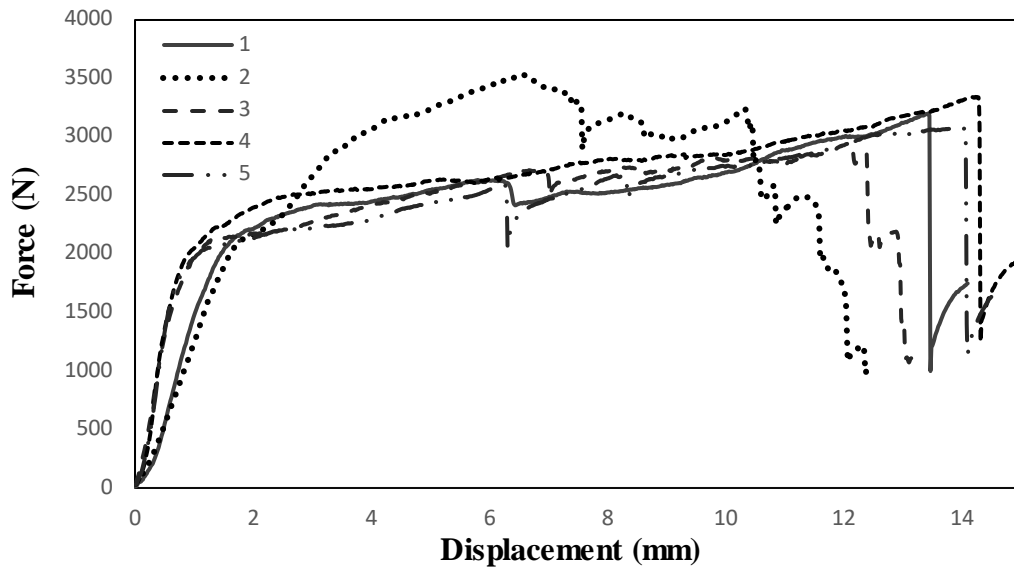


Figure 4.30. Force-displacement curves of composite sandwich structures under flexural loading (core thickness is 46 mm)

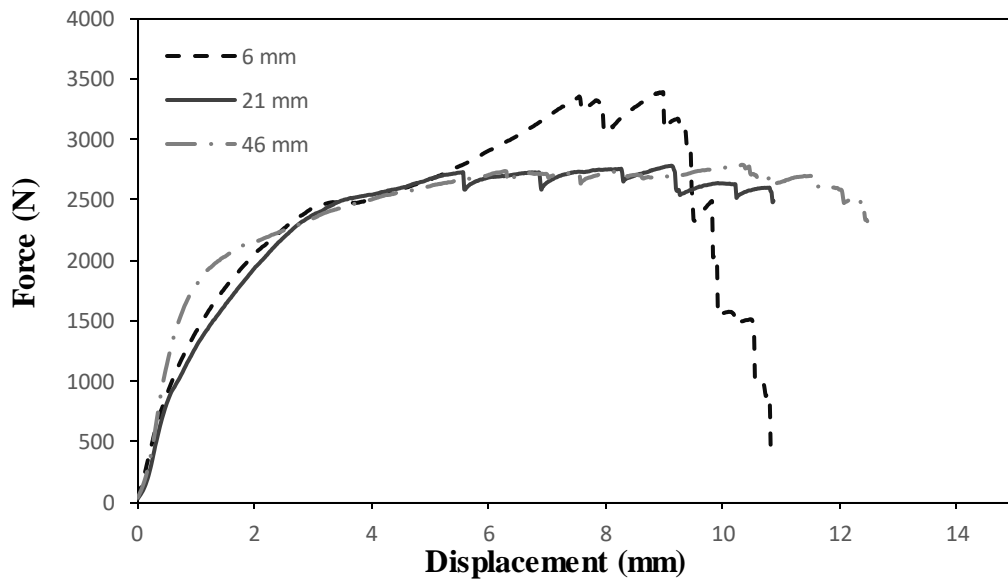


Figure 4.31. Comparison of typical flexural behavior of composite sandwich structures for various core thicknesses

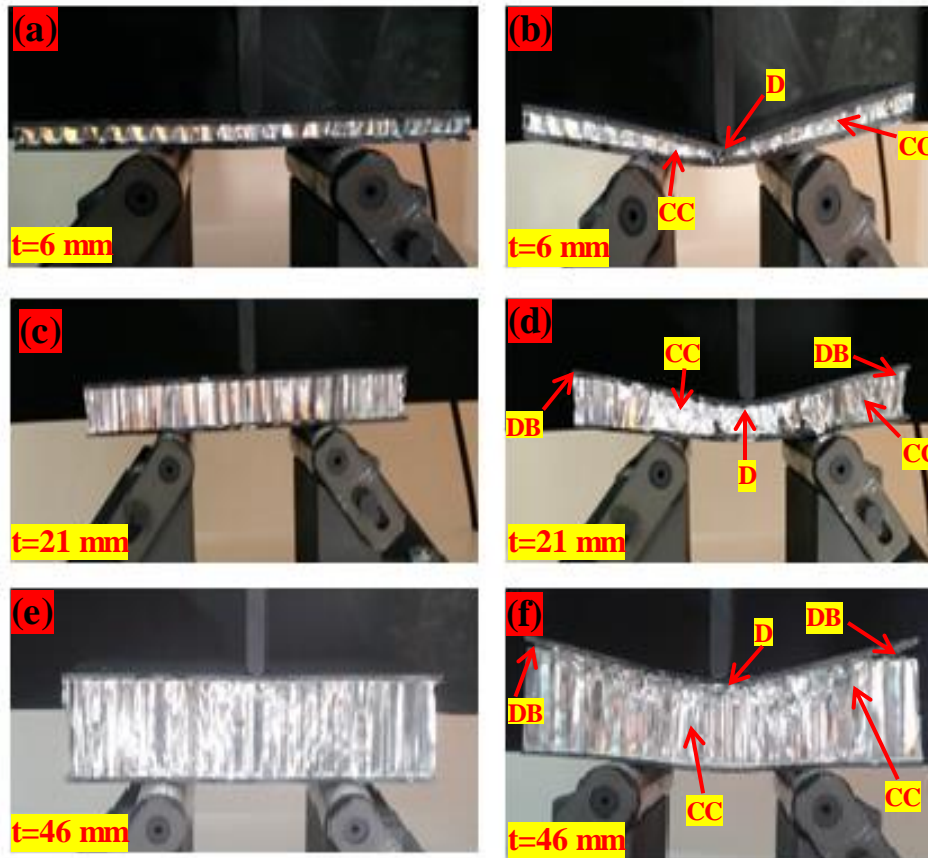


Figure 4.32. Images of flexural test specimens; before (a-c-e) and after (b-d-f) the tests (DB:debonding, CC: core crushing and D: delamination) (t is the core thickness in mm)

Table 4.10. Summary of the flexural test results of the composite sandwich structures

Core Thickness (mm)	Core Shear Stress (MPa)	Sandwich Beam Deflection (mm)	Panel Bending Stiffness (Pa.m ⁴)	Panel Shear Rigidity (N)	Face Sheet Bending Stress (MPa)
6	2.85 ± 0.22	14.91 ± 1.26	361.2 ± 38.8	14078 ± 556	52.0 ± 4.4
21	0.84 ± 0.08	2.07 ± 0.14	5047.4 ± 112.2	78905 ± 2754	15.9 ± 0.9
46	0.45 ± 0.03	0.76 ± 0.04	35261.6 ± 670.5	210852 ± 2647	8.8 ± 0.2

4.3.5. Mode-I Interfacial Peel Strength Values

Mode-I peel strength of the sandwich composites for various core thicknesses were measured as a function of the applied load and crack length. Figure 4.33 to 4.35 shows the force-displacement graphs of the Mode-I peel specimens. It was observed that the crack propagation is unstable resulting in sudden load drops as seen in the figure.

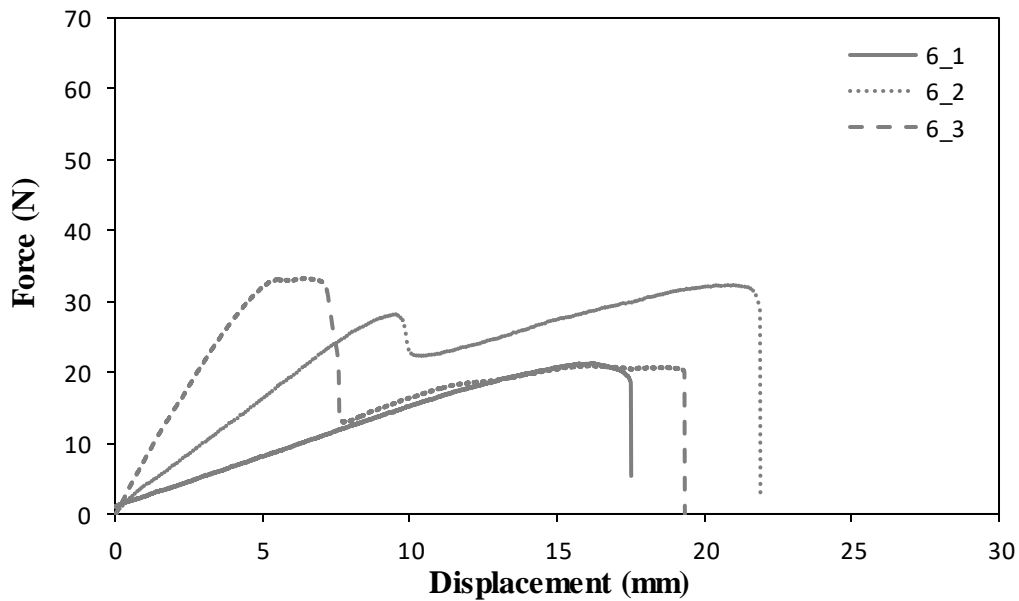


Figure 4.33. Force-displacement curves of composite sandwich structures under peel loading (core thickness is 6 mm)

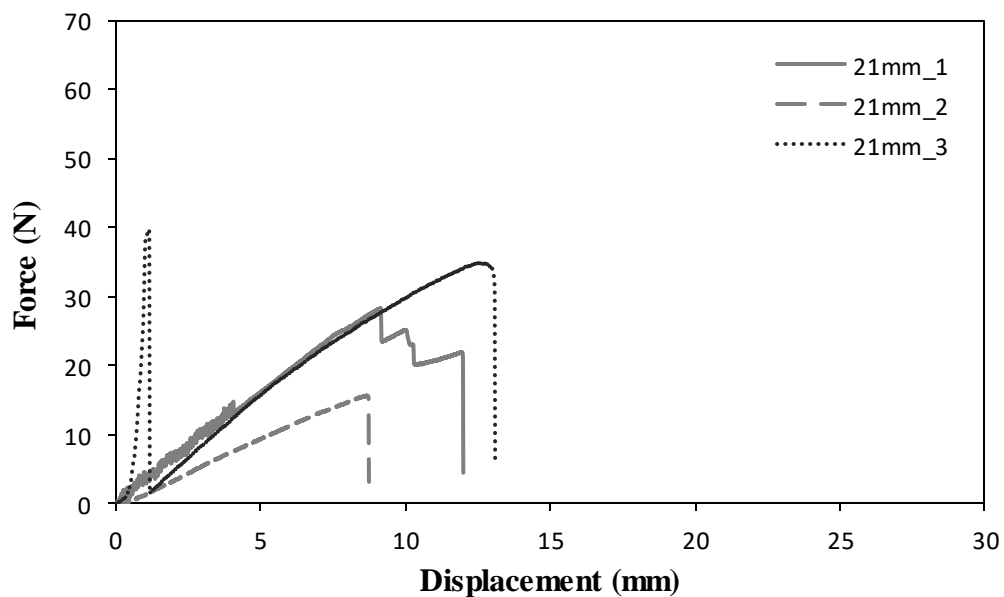


Figure 4.34. Force-displacement curves of composite sandwich structures under peel loading (core thickness is 21 mm)

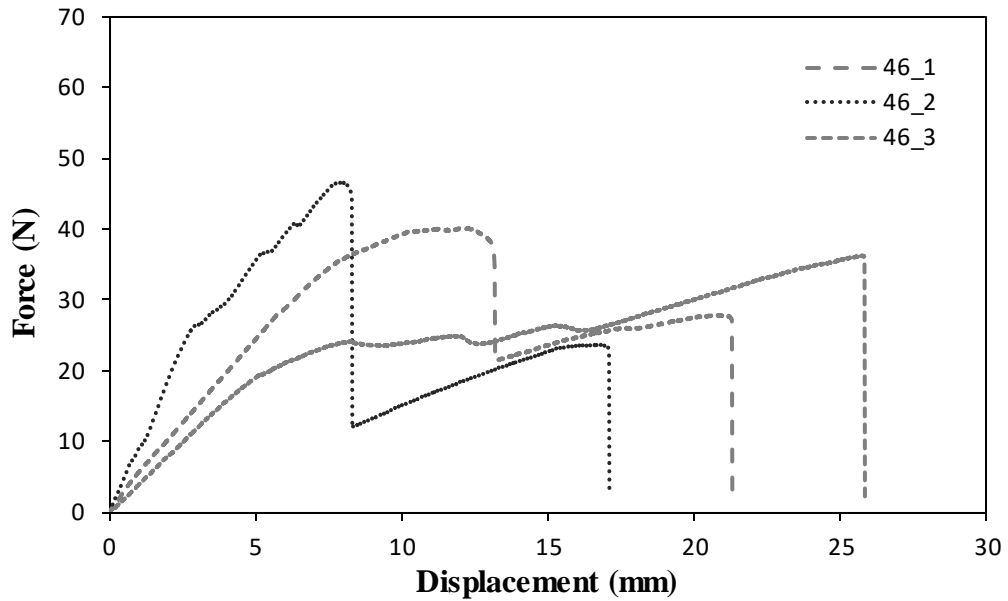


Figure 4.35. Force-displacement curves of composite sandwich structures under peel loading (core thickness is 46 mm)

The average peel strength values were calculated for various core thicknesses, respectively as summarized in Table 4.11. It was observed that there is no significant relation between the core thickness and applied force. Peel strength value is not related with the honeycomb core and cell wall thickness increments. A sudden and large crack growth was observed. Images of the test specimens under Mode-I loading are shown in Figure 4.36. The fracture surfaces of face sheet and core were examined by Scanning Electron Microscope (SEM) (Figure 4. 37).

Table 4.11. Summary of Mode-I peel strength values

Core Thickness (mm)	Peel Strength (N/mm)
6	1.15±0.26
21	1.12±0.48
46	1.69±0.93

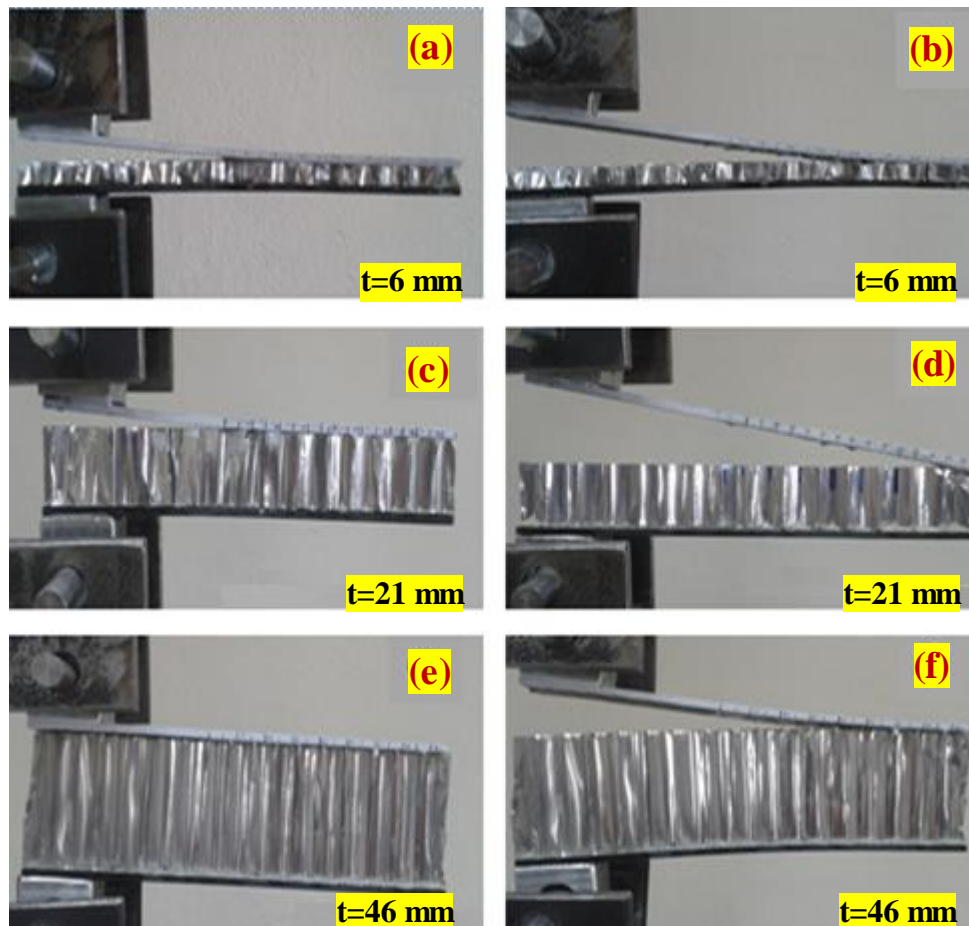


Figure 4.36. Mode-I peel test specimens; at the beginning (a-c-e) and during (b-d-f) the tests (t is the core thickness in mm)

It was observed that adhesive failure at the Al core/composite face sheet interface occurred. The spherical particles seen in the images are the filler materials existing in the adhesive. The failure surfaces seen on both side of face sheet and core material indicates that the failure occurred at adhesive layer. Adhesive material failed under Mode-I due to applied tensile stress. The smooth surfaces on the spherical fillers also indicate weak interface between filler and adhesive glue materials.

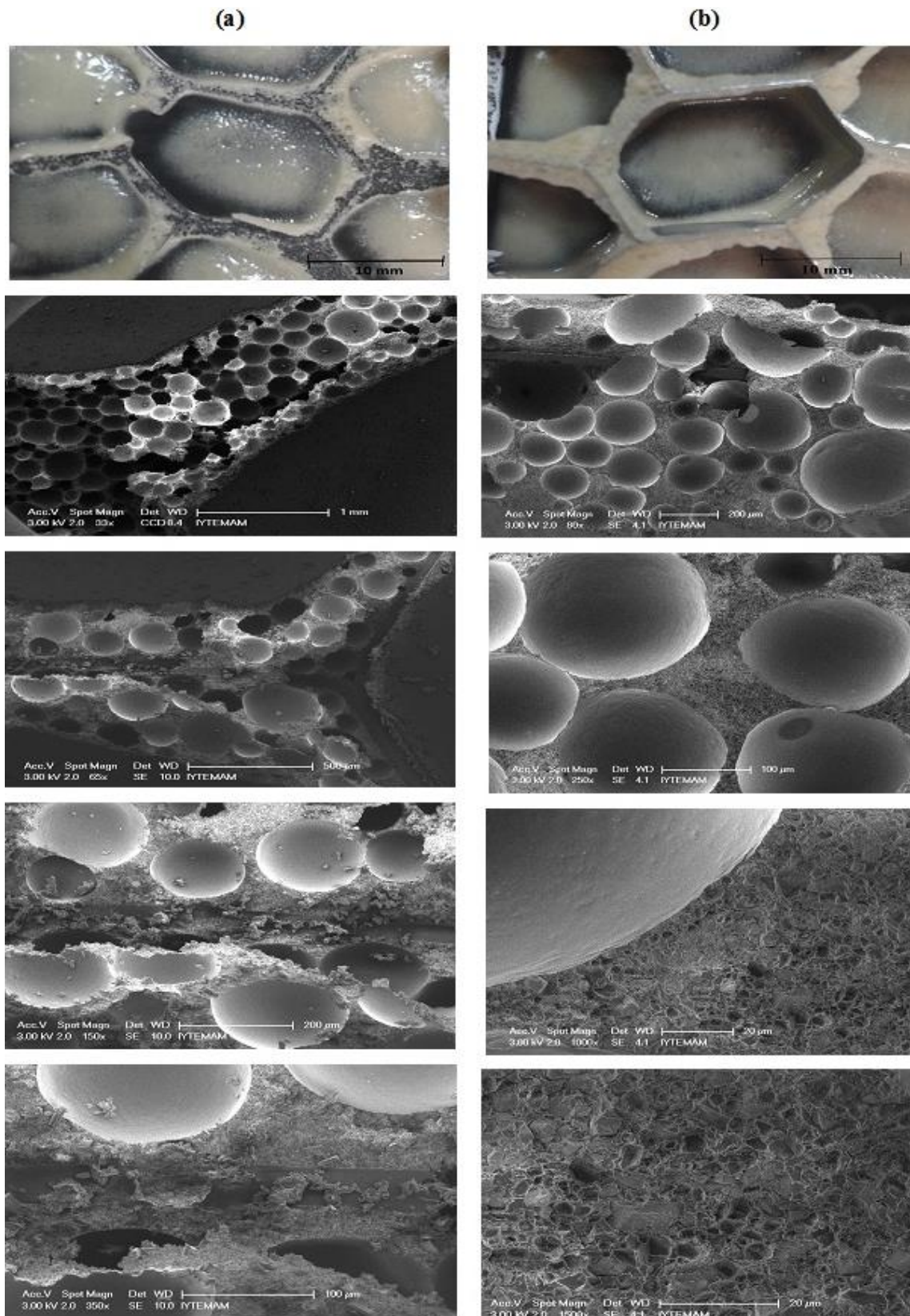


Figure 4.37. SEM fracture surfaces images of Mode-I test specimens; (a) the face sheet side, and (b) the core side of the specimen.

CHAPTER 5

CONCLUSION

In this study, composite sandwich structures composed of UD carbon fiber/epoxy face sheets and aluminum (Al) based honeycomb core were developed. Carbon fiber based face sheets were manufactured using vacuum infusion technique. Carbon fiber-epoxy/Al honeycomb core sandwich structures were laminated by adhesion technique with three different core thickness; 6, 21 and 46 mm to investigate the effects of core thickness on the mechanical properties of these structures. The mechanical behavior of the honeycomb core material and carbon fiber/epoxy face sheets were also determined according to relevant ASTM test standards.

The flatwise compression tests were carried out on the honeycomb core material. The results showed that the compressive strength and modulus of the core material increases with increasing thickness of the honeycomb. It was seen that honeycomb core cell walls buckled locally and densified with compression loading.

Tensile, compression, flexural and ILSS tests were carried out on the composite face sheet material. It was observed that the specimens failed with buckling, delamination and shear. The specimens had acceptable failure modes for all test methods.

For the sandwich structures, flatwise tensile, flatwise compression, edgewise compression, flexural and Mode-I peel tests were performed. It was observed that flatwise compression behavior and deformation of the composite sandwich structures with honeycomb core material are similar as the core material itself. It was also observed that the face sheets had no significant effect on the flatwise compressive properties of sandwich structures. The sandwich structures failed in different modes considering the core thickness; the core wall cells of the sandwich structure failed with buckling while the thicker cores failed with higher fraction of crushing under the same deformation. Energy absorption capacity increased with increasing core thickness of the composite sandwich structure due to the densification of the folded cell walls. During the edgewise compression tests, the face sheets of sandwich structure buckled, the interfacial debonding and core crushing was observed due to the shear at the interface

between the core and the face sheet laminate. The failure combination was collapse mode called “sandwich panel column buckling”. This collapse mode can be seen in thin structures which have lower crushing energy absorption. In thicker sandwich structures, the combination of global bending with core shear failure modes were observed and these sandwich structures contributed to the dissipation of the energy as well as higher average crushing load and compressive load uniformity. The complete failure occurred due to the core crushing followed by flexural cracking in the top face sheet. Although flexural cracks were observed at the top face of the sandwich beam, these cracks did not cause sudden failure due to the core crushing as in edgewise compression tests. Energy absorption capacity increased with core thickness increment. Final failure of the sandwich beam was due to compressive failure of the fiber composite skin followed by the debonding between the compressive skin and the core. As the core thickness increased, the amount of the core crushing and debonding at the interface increased. Three point bending test results showed that core shear stress, sandwich beam deflection and face sheet bending stress decreased while the panel bending stiffness and shear rigidity increased with the core thickness increment. Mode-I peel and flatwise tensile test results were not affected with the core thickness.

In summary, the core thickness was found to be a critical parameter for the flatwise and edgewise compressive and flexural behaviors of the composite sandwich structures, although it has no effect to the bonding between the constituents, as expected.

REFERENCES

- Adams, Donald F., 2006. Sandwich panel test methods. *High Performance Composites*, no. 5: 4-6. <http://www.compositesworld.com/> (accessed March 30, 2016).
- Advani S. and Hsiao K.T., 2012. *Manufacturing Techniques for Polymer Matrix Composites(PMCs)*, Woodhead Publishing Limited, Cambridge CB22 3HJ, UK.
- Aktay L., Johnson A.F., Kroplin B.H., 2008. Numerical modelling of honeycomb core crush behaviour, *Engineering Fracture Mechanics*, 75, 2616-2630.
- Amraei M. , Shahravi M., Noori Z. and Lenjani A., 2013. Application of aluminium honeycomb sandwich panel as an energy absorber of high-speed train nose, *Journal of Composite Materials* 0(0) 1-11.
- Ashab A.S.M., Ruan D., Lu G., Wong Y.C., 2016. Quasi-static and dynamic experiments of aluminum honeycombs under combined compression-shear loading, *Materials and Design*, 97, 183-194.
- Atas C. and Potoglu U., 2016. The effect of face-sheet thickness on low-velocity impact response of sandwich composites with foam cores, *Journal of Sandwich Structures and Materials*, 18(2), 215-228.
- Barbero E.J., 2011. *Introduction to composite material design*, second edition, CRC press, taylor and francis group, LLC.
- Bari D.D., Bajaj P.S., 2014. Theoretical flexural behavior of sandwich panel using composite materials, *International Journal Of Research in Engineering And Technology*, 03(04), 2319-1163, 826-830.
- Baştürk S.B., 2011. Development and mechanical characterization of anti-blast sandwich composites for explosive effect. *Izmir Institute of Technology, Thesis of PhD*.
- Callister W.D., 2006. *Materials Science and Engineering An Introduction*, 7 edition, Wiley Publishing.

- Campbell F. C., 2010. *Structural Composite Materials*, ASM International.
- Catapano A., Montemurro M., 2014. Optimal design of sandwich plates with honeycomb core. *Joint Conference on Mechanical, Design Engineering & Advanced Manufacturing*, Springer Verlag, pp.1-7, France.
- Cho J. U., Choi H. K., Lee S., Cho C. and Han M. S., 2013. Experimental study of the impact characteristics of sandwich composites with aluminum honeycomb cores, *International Journal of Automotive Technology*, 14(3), pp. 415-421.
- Coskun O. and Turkmen H.S., 2012. Bending fatigue behaviour of laminated sandwich beams, *Advanced Materials Research, Materials and Manufacturing Technologies*, XIV, 445, pp 548-553.
- Crupi V., Epasto G., Guglielmino E., 2013. Comparison of aluminium sandwiches for lightweight ship structures: Honeycomb vs. foam , *Marine Structures*, 30, 74-96.
- Daniel, I.M., 2009. Influence of core properties on the failure of composite sandwich beams, *Journal of Mechanics of Materials and Structures*,4, 7-8.
- Daniel, I.M. and Ishai, O., 1994. *Engineering mechanics of composite materials*, Oxford University Press.
- Donga A., 2011. Application of sandwich beam in automobile front bumper for frontal crash analysis. *Wichita State University Thesis of MS*.
- Eric Greene Associates, 1999. *Marine Composites*, Second edition, Eric Greene Associates, inc., Maryland, USA.
- Fan H., Yang L., Sun F., Fang D., 2013. Compression and bending performances of carbon fiber reinforced lattice-core sandwich composites, *Composites: Part A*, 52, 118-125.
- Frostig Y., 2005. Geometrical non-linear response of modern sandwich panels localized effects, *Sandwich Structures 7: Advancing with Sandwich Structures and Materials*.
- Gdoutos E.E., Daniel I. M., 2008. Failure modes of composite sandwich beams *Theoret. Appl. Mech.*, 35, 1-3, pp. 105–118, Belgrade.

- George T., 2014. Carbon Fiber Composite Cellular Structures, *University of Virginia Thesis of PhD*.
- Hasseldine B.P.J., Zehnder A.T., Keating B.D., Singh A.K. and Davidson B.D., 2015. Compressive strength of aluminum honeycomb core sandwich panels with thick carbon-epoxy facesheets subjected to barely visible indentation damage, *Journal of Composite Materials*, 0(0) 1–16.
- Hexcel , 2013. Hexcel Corporation, *HexPly 8552 epoxy matrix product data sheet* (accessed: March 14, 2016).
- HexWeb™, 2000. Honeycomb Sandwich Design Technology, <http://www.hexcel.com/> (accessed: March 14, 2016)
- HexWeb™, 1999. *HexWeb™ Honeycomb attributes and properties: a comprehensive guide to standard Hexcel honeycomb materials, configurations, and mechanical properties*, Report TSB 120, Hexcel Composites.
- Hoa S.V., 2009. *Principles of the Manufacturing of Composite Materials*, DEStech Publications Inc.
- Hollaway L.C and Head P.R. 2001. *Advanced Polymer Composites and Polymers in the Civil Infrastructure*, 1. Edition, Elsevier.
- Kaw A.K., 2006. *Mechanics of composite materials*, 2nd ed. Taylor & Francis Group LLC, CRC Press, Broken Sound Parkway NW,USA.
- Kessler M.R., 2004. *Advanced Topics in Characterization of Composites*, Trafford Publishing.
- Lee S.M., 1992. *Handbook of Composite Reinforcements*, John Wiley & Sons.
- Lindström A., 2007. Strength of Sandwich Panels Loaded in In-plane Compression, *KTH Engineering Sciences Licentiate Thesis*.
- Lokensgard E., 2008. *Industrial Plastics: Theory and Applications*, 219-220, Cengage Learning.

- Lu C., Zhao M., Jie L., Wang J., Gao Y., Cui X., Chen P., 2015. Stress Distribution on Composite Honeycomb Sandwich Structure Suffered from Bending Load, *Procedia Engineering*, 99, 405-412.
- Mallick P.K., 1997. *Composites Engineering Handbook*, CRC Press.
- Mamalis A.G., Manolakos D.E., Ioannidis M.B, Papapostolou D.P., 2005. On the crushing response of composite sandwich panels subjected to edgewise compression: experimental, *Composite Structures*, 71, 246-257.
- Manalo A.C., Aravinthan T. and Karunasena W., 2012. Mechanical properties characterization of the skin and core of a novel composite sandwich structure, *Journal of Composite Materials* 0(0) 1–16.
- Manshadi B.D., 2011. Biaxial Wrinkling of Thin-Walled GFRP Webs in Cell-Core Sandwiches. *Ecole polytechnique federale de Lausanne Thesis of PhD*.
- Miracle D.B. and Donaldson S.L., 2001. *ASM Handbook Vol. 1. Composites*. Ohio: The Materials Information Company, ASM International, USA.
- Mortensen A., 2007. *Concise Encyclopedia of Composite Materials*, Second edition, Elsevier, Amsterdam, Netherlands.
- Mozafari H., Molatefi H., Crupi V., Epasto G. and Guglielmino E., 2015. In plane compressive response and crushing of foam filled aluminum honeycombs, *Journal of Composite Materials*, 49(26) 3215-3228.
- Njuguna J., 2016. *Lightweight Composite Structures in Transport: Design, Manufacturing, Analysis and Performance*, Woodhead Publishing no. 5: 4-6.
- Paik J.K., Thayamballi A.K, Kim G.S., 1999. The strength characteristics of aluminum honeycomb sandwich panels, *Thin-Walled Structures* 35, 205-231.
- Park S-J., 2014. *Carbon Fibers*, Springer.
- Petras A., 1998. Design of Sandwich Structures. *Cambridge University Thesis of PhD*.
- Pilato L.A., Michno M.J., 2013. *Advanced Composite Materials*, Springer Science & Business Media.

- Prakash A.A., 2011. The Static, Impact and Vibration Behavior of FRP Honeycomb Core Sandwich Composites. *Anna University Thesis of PhD*.
- Rao K. K. and Rao K. J., 2014. Heat Insulation Analysis of an Aluminum Honeycomb Sandwich Structure, *IPASJ International Journal of Mechanical Engineering*, Volume 2, Issue 8, August 2014.
- Reddy J. N., 2004. *Mechanics of Laminated Composite Plates and Shells: Theory and Analysis*, Second Edition, CRC Press, USA.
- Russell B. P., Liu T., Fleck N. A., Deshpande V.S., 2011. Quasi-Static Three-Point Bending of Carbon Fiber Sandwich Beams with Square Honeycomb Cores, *Journal of Applied Mechanics*, Vol. 031008-8 78, May 2011.
- Schwartz M.M., 1997. *Composite Materials Properties, Nondestructive testing and Repair*, Volume 1, Prentice-Hall Inc.
- Sharaf T.A.M., 2010. Flexural Behaviour Of Sandwich Panels Composed of Polyurethane Core and GFRP Skins And Ribs. *Queen's University Kingston Thesis of PhD*.
- Shi S., Sun Z., Hu X., Chen H., 2014. Carbon-fiber and aluminum- honeycomb sandwich composites with and without Kevlar-fiber interfacial toughening, *Composites: Part A*, 67, 102-110.
- Shi S., Sun Z., Hu X., Chen H. 2014. Flexural strength and energy absorption of carbon Fiber-aluminumhoneycomb composite sandwich reinforced by aluminum grid, *Thin-Walled Structures*, 84, 416-422.
- Singh A.K., Davidson B.D, Hasseldine B. P.J and Zehnder A.T, 2014. Damage resistance of aluminum core honeycomb sandwich panels with carbon/epoxy face sheets, *Journal of Composite Materials*, 0(0) 1-18.
- Strong A.B., 2008. *Fundamentals of Composites Manufacturing-Materials, Methods, and Applications*, Society of Manufacturing Engineers, second edition, Michigan, USA.

- Strong A.B., 1989. *Fundamentals of Composites Manufacturing-Materials, Methods, and Applications*, Society of Manufacturing Engineers (SME), Michigan, USA.
- Sun Z., Shi S. Hu X., Guo X., Chen J., Chen H., 2015. Short-aramid-fiber toughening of epoxy adhesive joint between carbon fiber composites and metal substrates with different surface morphology, *Composites Part B*, 77, 38-45.
- Tuwair H. R., 2015. Development, testing, and analytical modeling of fiber-reinforced polymer bridge deck panels. *Missouri University of Science and Technology Doctoral Dissertations*.
- Vinson Jack R., 2005. *Sandwich structures: Past, present, and future, Advancing with Sandwich Structures and Materials Proceedings of the 7th International Conference on Sandwich Structures*, Denmark, 29-31 August.
- Vinson, Jack R., 1999. *The Behavior of Sandwich Structures of Isotropic and Composite Materials*, Technomic Publishing, USA.
- Vrabie M. and Chiriac R., 2014. Theoretical and numerical investigation regarding the bending behaviour of sandwich plates, *Bul. Inst. Polit. Iași, t., LX (LXIV)*, f. 4.
- Wadley H. N. G., 2006. *Multifunctional periodic cellular metals*, *Phil. Trans. R. Soc. A.*, 364, 31-68.
- Xiong J., Zhang M., Stocchi A., Hu H., Ma L., Wu L., Zhang Z., 2014. Mechanical behaviors of carbon fiber composite sandwich columns with three dimensional honeycomb cores under in-plane compression, *Composites: Part B*, 60, 350-358.
- Zhou G., Hill M. and Loughlan, J., 2006. Damage Characteristics of Composite Honeycomb Sandwich Panels in Bending under Quasi-static Loading, *Journal of Sandwich Structures and Materials*, 8, 55-90.